University of South Bohemia in České Budějovice

Faculty of Science

Identifying the Mode of Action for Bisphosphonium Salts – Potent Trypanosomatid Inhibitors

Master Thesis

Bc. Jan Martinek

Supervisor: RNDr. Alena Panicucci Zíková, PhD.

Institute of Parasitology, Biology Centre, ASCR, v.v.i.

Laboratory of Molecular Biology of Protists

České Budějovice, 2014

Martinek, J., 2013: Identifying the mode of action for bisphosphonium salts – potent trypanosomatid inhibitors. Mgr. Thesis, in English. – 47 p., Faculty of Science, University of South Bohemia, České Budějovice, Czech Republic.

Annotation

Two new benzophenone-derived bisphophonium salts were tested in *Leishmania donovani* and *Trypanosoma brucei*. In this study the effects of these compounds on succinate dehydrogenase, ATP synthase and mitochondrial membrane potential were explored to elucidate the mode of action.

Prohlašuji, že svoji diplomovou práci jsem vypracoval samostatně pouze s použitím pramenů a literatury uvedených v seznamu citované literatury.

Prohlašuji, že v souladu s § 47b zákona č. 111/1998 Sb. v platném znění souhlasím se zveřejněním své diplomové práce, a to v nezkrácené podobě elektronickou cestou ve veřejně přístupné části databáze STAG provozované Jihočeskou univerzitou v Českých Budějovicích na jejích internetových stránkách, a to se zachováním mého autorského práva k odevzdanému textu této kvalifikační práce. Souhlasím dále s tím, aby toutéž elektronickou cestou byly v souladu s uvedeným ustanovením zákona č. 111/1998 Sb. zveřejněny posudky školitele a oponentů práce i záznam o průběhu a výsledku obhajoby kvalifikační práce. Rovněž souhlasím s porovnáním textu mé kvalifikační práce s databází kvalifikačních prací Theses.cz provozovanou Národním registrem vysokoškolských kvalifikačních prací a systémem na odhalování plagiátů.

V Českých Budějovicích 25. dubna 2014

.....

Jan Martinek

Acknowledgements

Na tomto místě bych chtěl nejvíce poděkovat svým školitelům Aleně Zíkové a Brianu Panicucci za příležitost u nich pracovat, za odborné vedení, trpělivost a ochotu se vším pomoci. Dále pak všem členům laboratoře funkční biologie protist především Míše, Káje, Davidovi a Evče za cenné rady, zodpovídání mých dotazů a vytvoření skvělého pracovního prostředí. Dále také prof. Harry de Koningovi za poskytnutí inhibitorů použitých v této práci. Za podporu děkuji svým přátelům Janče, Martinovi a Věrce. Taktéž své rodině nejen za morální podporu ale i za finanční pomoc.

Table of contents

1 Introduction

1.1 Trypanosomatids

Trypanosomatids are single celled eukaryotic parasites. These organisms belong to the class Kinetoplasta, phylum Euglenozoa, kingdom Excavata. In addition to the organelles commonly found in most eukaryotic cells, these flagellated protists also posses a modified peroxisome called the glycosome which harbors most of the enzymes for glycolysis. These membrane-bounded organeles play an important role mainly in the bloodstream form (BF) of *Trypanosoma brucei* (*T. brucei*). Glycosomes are extensively remodeled during differentation between BF and procyclic form (PF). However little is known how these organelles originated (Gualdrón-López *et al.*, 2012). Interestingly, trypanosomatids only contain a single extended mitochondrion that runs the length of the entire cell. Furthermore these evolutionary ancient parasites are named after the unique electron dense staining in their mitochondria, which represents their complex mitochondrial DNA organized into concatenated circles called the kinetoplast. These parasites are responsible for several diseases in humans and livestock, most of which lead to death if untreated. Of particular importance are the genera *Leishmania* and *Trypanosoma* (Roberts *et al.*, 2009).

1.1.1 *Leishmania*

These heteroxenous parasites are mainly located in South America, Central Africa and south east Asia (Figure 1). Acording to some studies, about 300 million people are at risk, with about 1 million new cases recorded worldwide every year, culminating in 12 million people already infected (Dostálová and Volf, 2012).

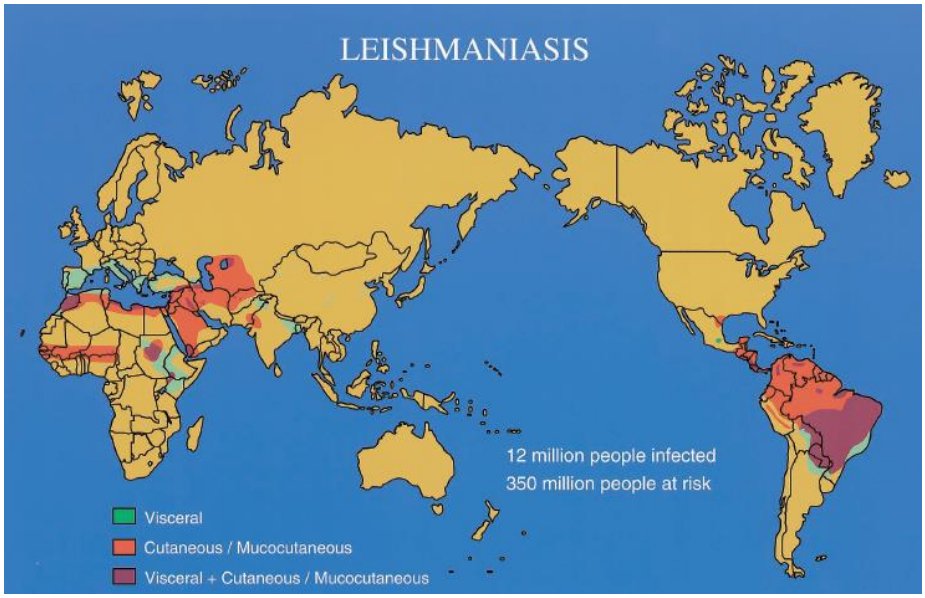

Figure 1. The occurence of 3 types of leishmaniasis in the world (Handman, 2001).

Leishmania go through a digenetic life-cycle as they alter between a mammalian host and an insect vector. They are transmitted by phlebotomine sand flies from the family Psychodidae. The intricate life cycle of *Leishmania* consists of several stages (Figure 2). First, the immobile amastigotes are ingested from the blood of a mammalian host by Phlebotomines. Once in the midgut of the sand fly, they are trigerred by the temperature and pH changes to divide and transform into motile, slender promastigotes. This allows them to reach the esophagus, pharynx and buccal cavity from where they can be transfered to a new host. In the human body, *Leishmania* have a pronounced tropism for macrophages, where they divide by binary fision. These immune cells are eventually killed by the parasite which in turn is engulfed by another macrophage.

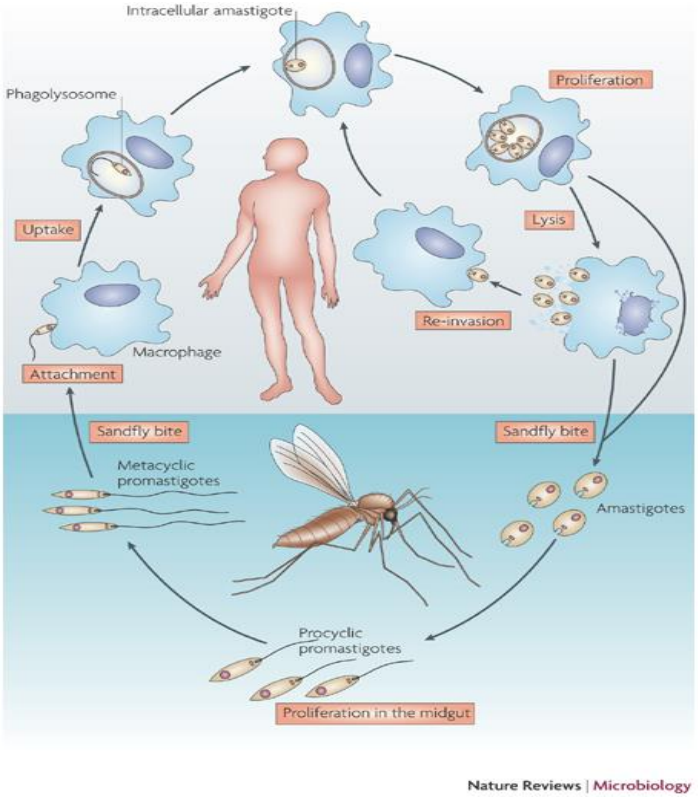

Figure 2. Life cycle of Leishmania donovani (Chappuis et al., 2007).

The symptoms of leishmaniasis are based on which species are the infecting agents. Basically two main forms of the disease exist: cutaneous (CL) and visceral (VL). More than 50% of new cases are cutaneous leishmaniasis. Lesions appear near the site of the sand fly bite and are usually self-healing, although some species cause non-healing cutaneous disease (*Leishmania tropica*, *aethiopica* or *mexicana amazonensis*). Imunocompromised or susceptible patients can be affected by a rare but severe form: disseminated cutaneous or diffuse cutaneous leishmaniasis. Even when the disease was completely cleared, a small percentage of these cases can develop into mucocutaneous form (MCL), when the metastatic lesions destruct mucous membranes. Mechanisms how the lesions are formed are poorly understood (possible role of leishmania RNA virus). 90% of CL is observed in Afghanistan, Middle East and South America. The most severe and often fatal form is VL (kala-azar). It is caused mainly by *Leishmania donovani* (*L. donovani*) in India, sub Saharan Africa, Asia and by *Leishmania infantum* in the Americas and the Mediterranean basin. The parasite infects phagocytic cells within spleen, lymph nodes, liver and bone marrow which results in fever, hepatosplenomegaly, anemia or thrombocytopenia. Unfortunately no effective vaccine against leishmaniasis has been developed yet (Kedzierski, 2011; Esch and Petersen, 2013; Handman, 2001).

1.1.2 *Trypanosoma*

Many species are included in this genera. Basically they can be divided into two big groups based on how they develop in the insect vector Stercoraria and Salivaria.

The parasite *Trypanosoma cruzi* from the group Stercoraria can be found in South and central America where it is responsible for causing Chagas disease (american trypanosomiasis). In addition, there are emerging endemic areas witha lot of cases in the USA, Canada and Spain. Humans are usually infected when they come into contact with infected feces of triatome bugs. According to WHO (2010), 10 million people are infected and around 25 million are at risk. Most of the patients in accute or chronic phase are asymptomatic. Symptoms can develop after many years of dormancy. Also up to 40% of chronically infected patients develop cardiac alterations, for example dilated cardiomyopathy (Carabarin-Lima *et al.*, 2013; Nunes *et al.*, 2013).

From the group Salivaria, *T. brucei* is responsible for the economically important disease nagana (AAT animal african trypanosomiasis), which results in livestock wasting. *T. brucei gambiense* and *T. brucei rhodesiense* are named after the African geographical regions they are most predominantly found and are also members of Salivaria, but these subspecies are the causative agents for human african trypanosomiasis (HAT) in 36 sub-Saharan Africa countries (Roberts *et al.*, 2009).

Trypanosoma evansi are special species derived from a *T. brucei* strain that partially lost their kDNA (dyskinetoplastik-DK) and thus lost gRNA genes needed for the transformation of BF to PF. These monoxenous parasites are transmitted mechanically and because they are not dependent on the tsetse vector they can spread out of Africa (Asia, Central South America). DK's are characterised by the loss of A6 expression, a putative subunit of complex V important in maintaining the mitochondrial membrane potential (mmp). To compensate that, DK parasites contain a mutated γ subunit of complex V (Lai *et al.*, 2007; Schnaufer, 2010; Lun 2010).

1.1.2.1 Human african trypanosomiasis

The prevalence of the disease has changed quite significantly in the last 100 years. In 1960's the transmission rate was quite low but due to a lack of awareness the number of new cases unfortunately started to rise again (Simarro *et al.*, 2008). Statistics say that at least 60 million people are at risk and every year 10 000 new cases appear mainly in central and east central Africa (*Trypanosoma rhodesiense*), central and west central

Africa (*Trypanosoma gambiense*) which accounts for 98% of all reported cases (Figure 3).

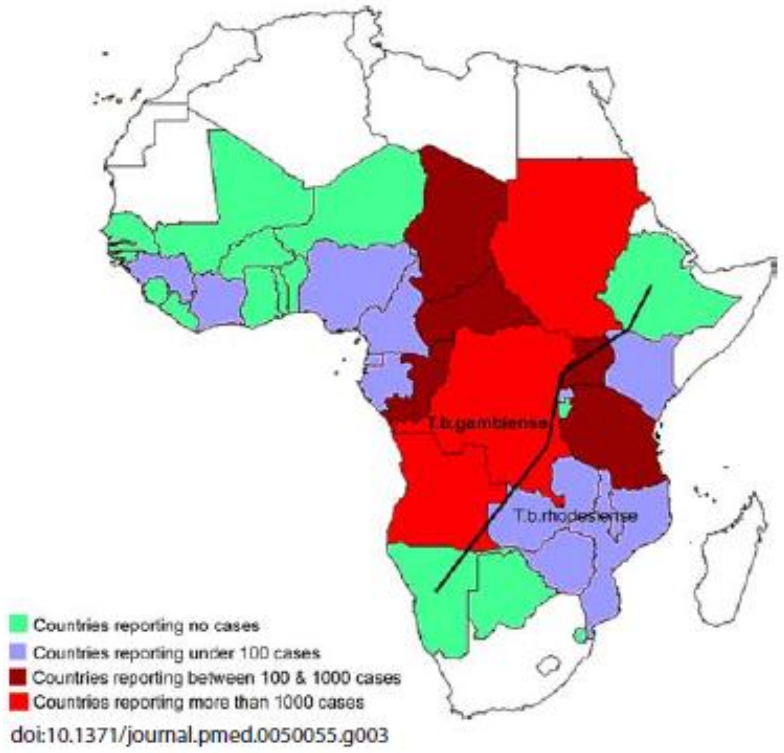

Figure 3. Map of Africa showing the epidemiological status of countries considered endemic for the disease (Simarro et al., 2008).

The highest prevalence of the disease was observed in the Democratic republic of the Congo (Hasker *et al.*, 2008). The occurence of sleeping sickness corelates with the presence of the Glossina tsetse flies, which are the trypanosoma insect vectors required to complete their digenetic life cycle (Simmaro *et al.*, 2008). Simply described, the two life stages of *T. brucei* are the PF found in the insect vector and the BF that replicates in the mammalian bloodstream as shown in Figure 4. Humans become infected when trypansomes that have migrated from the midgut to the salivary glands of the tsetse fly are transferred to the mammalian bloodstream by a tsetse bite. It is in this glucose rich environment that the parasite is able to reside extracellularly by utilizing a unique system to shed and replace its uniform glycoconjugated protein coat (Hall *et al.*, 2013).

Symptoms of the disease can be divided into two periods early and late. In the early period, the first symptoms appear 1-3 weeks after an insect bites. These include headache, nausea, joint pain, weight loss, fatigue and fever alternating with stiffness. These symptoms can often be quite mild and dissipate quickly, leading many patients to be mistakenly diagnosed with the common flu. However, some patients will gradually

display lymphadenopathy, an enlarged spleen or liver, heart disorders, ocular inflammation, endocrine disorders, and fertility problems. Late stages of the disease manifest once the trypanosomes are able to cross the blood brain barrier and cause damage to the central nervous system (CNS), resulting in mental disorders, musculoskeletal disorders, sensory perception, and abnormal reflexes. Most patients exhibit typical sleep disorders, such is the name given this debilitating disease (Barrett et al., 2003).

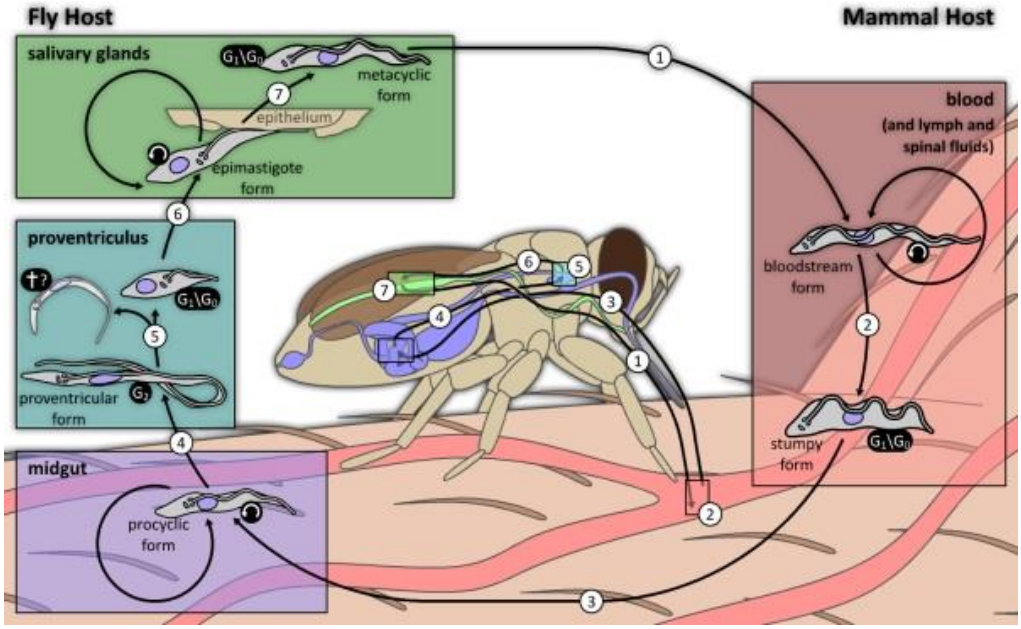

Figure 4. Life cycle of *T. brucei*.
(http://www.richardwheeler.net/contentpages/image.php?gallery=Scientific_Illustration&img=Trypanosome_Life_Cycle&type=jpg)

The classical method employed for screening highly susceptible populations is microscopy of blood, lymph node aspirate and tissue fluid. Furthermore, sleeping sickness can be diagnosed through a series of serological tests and DNA hybridization (Brun *et al.*, 2010).

Untreated trypanosomiasis ends fatally. Unfortunately, it is not possible to vaccinate against this lethal disease because as mentioned previously, the infectious trypanosomes are constantly able to change their surface antigens as the host develops specific antibodies Therefore, we must rely on chemotherapeutics to treat HAT, but the current drugs are far from perfect as they often require travel to a hospital, where prolonged stays are necessitated because of the prolonged and complicated drug administration. Furthermore, many of these expensive drugs have very toxic side effects, often lack efficacy against the second stage of the disease and there are increasing reports

of resistance to these drugs. Thus, searching for drugs with better properties has a high priority (Barrett and Croft, 2012; Kennedy 2013).

1.2 Bisphosphonium salts

One of the more promising drugs against Leishmaniasis and Trypanosomiasis are the new benzophneone-derived bisphosphonium salts. Already in 1979, the killing activity of benzyltriphenylphosphonium salts was observed in *T. brucei* (Kinnamon *et al.*, 1979). But due to a lack of information and experience the research was discontinued for several years.

The new bisphosphonium salts were synthesized in 2010 by the laboratory of Christophe Dardonville. They showed that these compounds have strong antileishmanial activity and proposed that they target respiratory complex II (cII, succinate dehydrogeanse) in the mitochondria based on phenotypical analyses demonstrating that treated parasites have a dramatically swollen mitochondrion, decreased levels of adenosine triphosphate (ATP), decreased mmp and an inhibition of oxygen consumption when using succinate as a substrate (Luque-Ortega, 2010).

In this study we analyzed two bisphosphonium salts CD38 and AHI-9. The structure and difference between those two are shown in Figure 5.

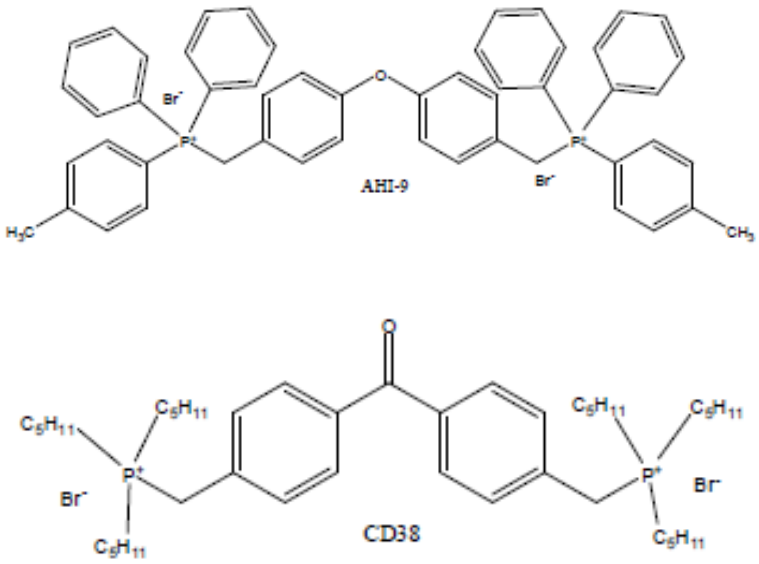

Figure 5. The structure of CD38 and AHI-9 (Alkhaldi PhD thesis, 2012).

These compounds most likely accumulate in the mitochondria because like other lipophilic cations, they have a greatly delocalized and shielded charge that allows them to

pass through biological membranes and concentrate in the mitochondrial matrix, which has a negative charge (Ross *et al.*, 2008). This chemical attribute could possibly be an advantage for the delivery of the drug, especially during treatment of the second stage of trypanosomiasis because the compounds could penetrate into the CNS. Furthermore, while these salts were active against trypansomes at a low micromolar concentration, they exhibited very low toxicity when tested on human embryonic kidney (HEK) cells. . Importantly, they also did not exhibit cross resistance with any currently used drugs (diamidines, arsenical trypanocides), which is significant for any new potential therapeutic (Alkhaldi, 2012).

1.3 Metabolism changes in *T. brucei* PF to BF

Trypanosomes not only undergo structural changes during their life cycle, but also changes in metabolism, which is quite obvious when they are transported between environments with different nutrients and oxygen availability. In spite of that, they have to adapt to these new conditions.

All trypanosomatids use carbohydrates as a substrate for their energy metabolism (Morales *et al.*, 2009). In a process called glycolysis, which takes place in specialised organelles called glycosomes, carbohydrates are mainly reduced to pyruvate. PF *T. brucei*, transport pyruvate into the mitochondria, where it is catabolized by the Krebs cycle into carbon dioxide. During this cycle, the resulting reducing equivalents, NADH and $FADH_2$, are subsequently oxidized by the respiratory chain. This flow of electrons to oxygen enables the respiratory complexes to pump protons into the inner membrane space, effectively creating a proton gradient (the mmp) that is then used for the generation of ATP by complex V (Figure 6) (Bringaud *et al.*, 2006).

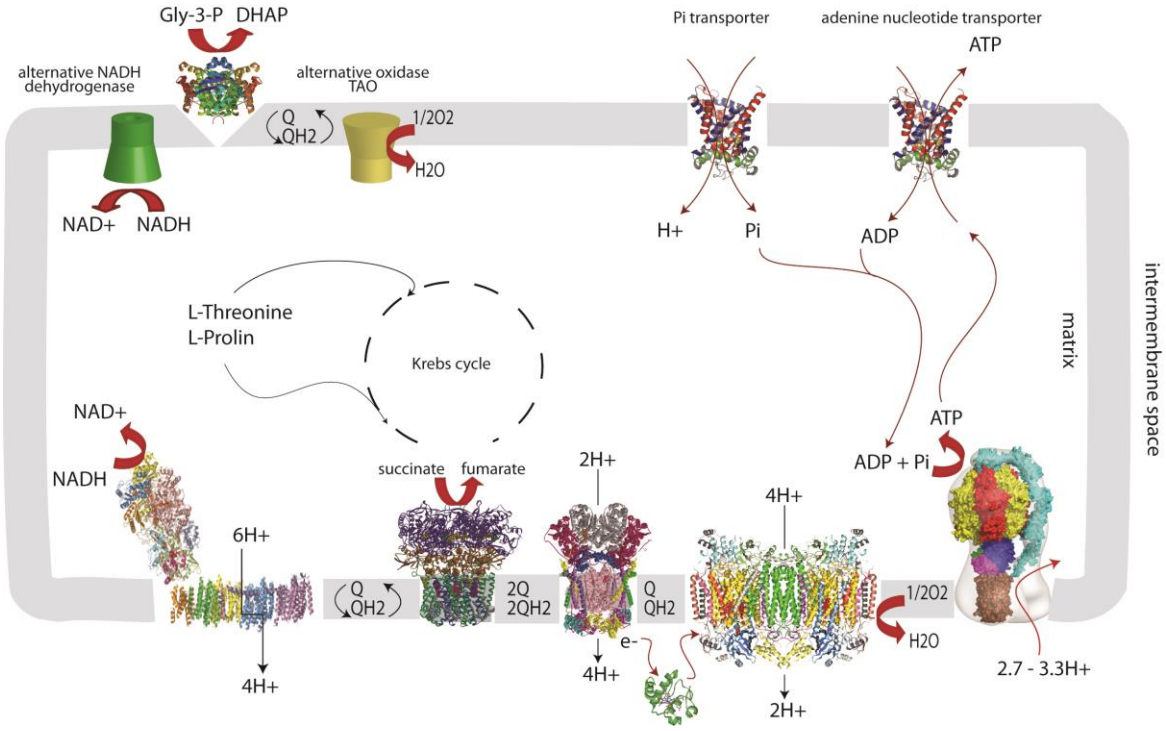

Figure 6. Scheme of the respiratory chain in *T. brucei* PF.

BF of *T. brucei* posses less developed mitochondria with almost no cristae. It lacks a functional cytochrome mediated respiratory chain and most of the Krebs cycle enzymes, so glycolysis is the main source of energy. Oxygen is now reduced by the alternative oxidase (TAO) and the mmp is maintained by the hydrolytic activity of the F_oF_1-ATPase (Tielens and Hellemond, 1998; Nolan and Voorheis 2000).

1.4 Mode of action of bisphosphonium salts

It has been shown that bisphosphonium drugs have leishmanicidal and trypanocidal activities. Moreover, these compounds have an inhibiting effect on BF *T. brucei*, resulting in the death of the parasites. However, BF cells are missing key functional components of the respiratory chain, which has rendered succinate dehydrogenase nonessential in the infectious stage of the parasite. Therefore, the mode of action of the bisphosphonium salts is unlikely to be respiratory complex II in BF *T. brucei* as it is suggested for *Leishmania*. Hence, we tested these compounds on both life cycles of *T. brucei* to help provide more insight into the mode of action for these potent inhibitors.

2 Aims

- Determine the relative abundance of assembled succinate dehydrogenase complexes and their overall activity levels in trypanosomatids.
- Generate and verify the efficiency of RNAi cell lines to knock-down the expression of succinate dehydrogenase subunit 1 in *T. brucei* PF and BF.
- Determine the importance of succinate dehydrogenase on the mmp in PF *T. brucei.*
- Measure the mmp and activity of respiratory complex II in *L. donovani*, both stages of *T. brucei* and a diskinetoplastid strain both before and after treatment with bisphosphonium salts.
- Measure the ATP synthesis and hydrolysis activities of the F_oF_1-ATP synthase in PF *T. brucei* both before and after treatment with the antitrypanocidal drugs.

3 Methods

3.1 Cell lines and cultivation

T. brucei Lister strain 427 PF (wild type strain) were cultivated in a glucose enriched SDM-79 media with 10% fetal bovine serum (FBS) at 25°C. *T. brucei* WT 427 BF and DK 164 were grown in HMI-9 with 10% FBS at 37°C. *L. donovani* promastigotes were cultured in M-199 media with 10% FBS at 27°C.

3.2 Western blotting

3.2.1 Principle of western blotting

This method is used for protein identification. First proteins have to be resolved by sodium dodecyl sulfate-polyacrylamide gel electrophoresis (SDS-PAGE). The SDS coats each protein, providing an overall negative charge that denatures the protein. The proteins are then repelled from the anode and migrate through the pores in the polyacrylamide gel. This serves to resolve the proteins based on their size as the smaller proteins move more quickly through the gel. For stability, the proteins are then transferred by a current onto a PVDF membrane in a wet apparatus. It is then possible to identify proteins of interest by allowing a specific primary antibody to bind to the membrane. This interaction is then detected by adding a secondary antibody that recognizes the species of the primary antibody. Importantly, the secondary antibody is fused to an enzyme that when provided with the appropriate substrate provides a chemiluminescent signal that is detected on a BioRad ChemiDoc instrument (Yang *et al.*, 2012)

3.2.2 SDH steady state levels in trypanosomatids

Mitochondrial enriched organellar fractions were isolated from trypanosomatids to enhance western blot detection of the steady state of subunit 1 from succinate dehydrogenase. $2{,}5x10^8$ cells of each cell line were harvested by spinning down the cells at 1300xg for 10 minutes at 4°C. Pellets were washed in PBS-G (5,6 mM $Na_2HPO_4x12H_2O$, 3,6 mM $NaH_2PO_4x2H_2O$, 0,145 M NaCl, 3,3 mM glucose) and

resuspended in 1.5ml of an ice-cold hypertonic solution called NET (0.15M NaCl, 0.1M EDTA, 10mM Tris-HCl pH 8.0) The cells were then spun for 10 minutes at 13200rpm at 4°C and resuspended in 1,4 ml of the hypotonic solution DTE (1mM Tris-HCl pH 8.0, 1mM EDTA). The swollen cells were then disrupted by passing them twice through a 25G needle. Immediately, sucrose was added 0,2M to return the lysed cells to an isotonic buffer, preventing further disruption of the isolated organelles. The lysed cells are then spun down at 13200rpm at 4°C for 10 minutes, which results in the clearing of the soluble cytoplasmic fraction. The organellar pellet was then resuspended in 500ul of STM (250mM sucrose, 20mM Tris pH 8.0, 2mM $MgCl_2$) and 1,5ul of 1M $MgCl_2$ and 2,5ul of DnaseI were added. This Dnase reaction was allowed to proceed on ice for 1 hour before it was finally stopped by adding 500ul of cold STE (250Mm sucrose, 20mM Tris pH 8.0, 10mM EDTA). The mitochondrial enriched organellar fraction was isolated after the sample was spun at 4°C for 10 minutes at 13200rpm. This wash step was repeated twice more. The protein concentration was measured by a Bradford assay.

The crude mitochondrial preparations were prepared for SDS-PAGE analysis by resuspending them in PBS (5,6 mM $Na_2HPO_4x12H_2O$, 3,6 mM $NaH_2PO_4x2H_2O$, 0,145 M NaCl) and SDS page loading dye (63 mM Tris Hcl, 10 % Glycerol, 2 % SDS, 0.0025 % Bromophenol Blue, pH 6.8) at a 2:1 ratio. Samples were boiled at 97°C for 7 minutes to further denature the proteins. 50ug of protein from each cell line was loaded along with a page ruler prestained marker (Thermo Scientific) on a stain free gel (BIO-RAD). Proteins from the gel were transfered to a PVDF membrane by applying 90V for 90 minutes. The membrane was blocked over night in a 5% milk solution in 1xPBS-T (5,6 mM $Na_2HPO_4x12H_2O$, 3,6 mM, $NaH_2PO_4x2H_2O$, 0,145 M NaCl, 0,05% Tween). The membrane was probed for 1 hour with a 1:1000 dilution of the SDH1 polyclonal rabbit antibody. The antibody was raised against the *T. brucei* SDH1 peptide (Figure 7).

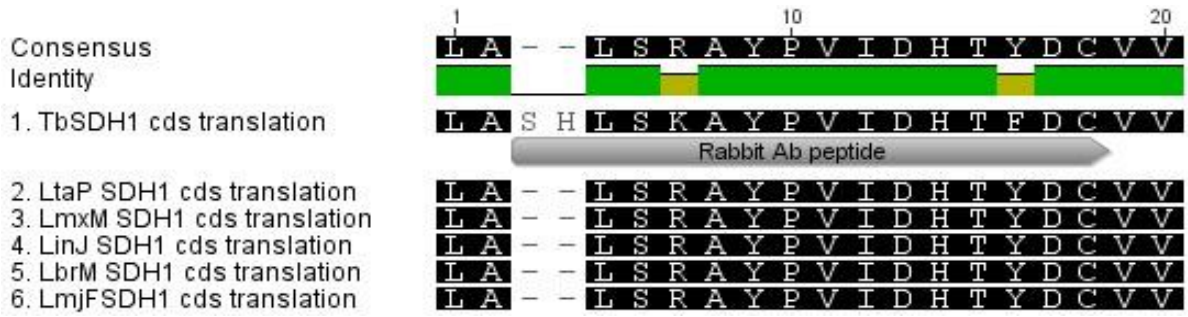

Figure 7. Polyclonal SDH1 antibody was raised against a specific *T. brucei* peptide. Alignment with *Leishmania tarentolae, L. mexicana, L. infantum, L. braziliensis* and *L. major*. Made in Geneious software.

The membrane was washed 3x10 minutes with PBS-T and then probed for 1 hour with a secondary anti-rabbit antibody diluted 1:2000. After washing the membrane for 3x10 minutes, an enhanced chemiluminiscent substrate (ECL) was added to the membrane and the signal was captured by the chemiluminiscence machine (BIO-RAD ChemiDoc^{TM} MP Imaging System).

3.2.3 Native assembly of complex II in trypanosomatids

Since we want to study whole protein complexes, we need to perform clear native PAGE instead of SDS-PAGE. No charged dye is applied, so the native proteins separate based on their size and charge.

Crude mitochondria were isolated as described previously and the protein concentration was determined by a Bradford assay. Mitochondria were resuspended in a digitonin lysis buffer (100 ul to 1 mg of the protein) (2mM ACA, 50mM Imidazole-HCl pH 7,0, 1mM EDTA, 50mM NaCl, pH 7,0) and digitonine was added (4mg of digitonine to 1 mg of the protein). The samples were incubated 1 hour on ice and then spun at 4°C for 30 minutes at 13200rpm.

The protein concentration was measured again after the lysis and equal amounts of protein (50ug) were loaded on a (3%-12%) polyacrylamide gradient gel. The native protein samples were run for 2-3 hours at 100V in an anode (50mM Tricine, 7,5mM Imidazole pH 7,0, 0,05% deoxycholin, 0,02% dodeclymaltoside) and cathode buffer (25mM Imidazole). After the proteins were resolved by PAGE, they were transfered to a stable nitrocelulose membrane by applying 20V over night. The marker was separated and put in Ponceau S (Sigma) to visualize the ladder. The rest of the membrane was then probed with a primary SDH1 antibody (1:1000 dilution) and a goat anti-rabbit secondary antibody (1:2000 dilution).

3.3 Succinate ubiquinone:oxidoreductase activity assay

We implemented an *in vitro* assay to biochemically measure the activity of succinate dehydrogenase. 5ul of a crude mitochondrial lysate (3000µg/ml) was added to 1ml of an SDH solution (25mmol/l KPi ph7,2, 5mmol/l $MgCl_2$, 20mmol/l sodium succinate) containing specific inhibitors of other respiratory complexes (0,0002% Antimycin, 2mM KCN) and 50uM DCIP which act as the electron acceptor, and changes from a blue

colour to colourless. Similar cuvettes also contained 1mM malonate, a specific inhibitor of SDH, as a negative control. The samples were thoroughly mixed by pipetting and the absorbance was measured at 600nm for 5 minutes at 30°C on the spectrophotometer (Shimadzu UV-1601) when the reaction was started by adding 65uM coenzym Q_2. Specific succinate ubiquinone:oxidoreductase activity of kinetoplastid lysate was calculated from the amount of reduced coenzym Q_2 in 1 minute and related to the amount of the protein in the sample.

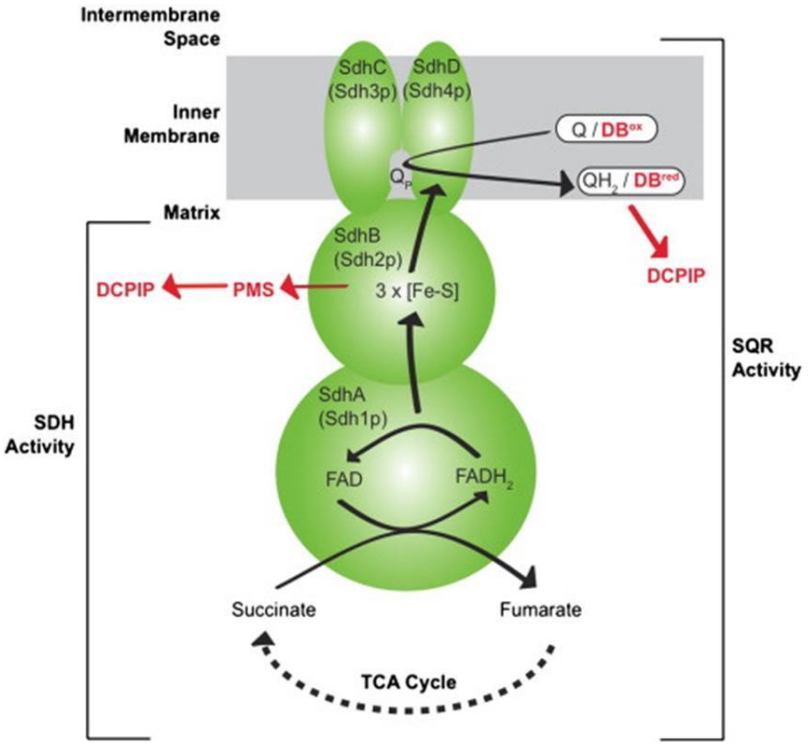

Figure 8. Scheme of succinate dehydrogenase structure and the route of passing electrons. Two types of complex II activities can be measured. The SDH activity is determined when electrons from the substrate succinate pass through only the first two subunits (A and B) before reducing phenazine methosulfate and the colorimetric dye dichlorophenolindophenol. SQR activity is measured when electrons continue from subunit B to the membrane bound subunits (C and D), before reducing ubiquinone and dichlorophenolindophenol.DCIP – dichlorophenolindophenol, PMS - phenazine methosulfate, Q – ubiquinone, QH2 – ubiquinol, SQR – succinate ubiquinone:oxidoreductase (http://www.sciencedirect.com/science/article/pii/S0005272812001478).

3.4 Generation of RNAi cell line

3.4.1 RNA interference

RNAi is a biological process enabling the specific degradation of a targeted mRNA using double-stranded RNA (dsRNA). This powerful method is employed to examine the functions of genes in several organisms. In *T. brucei*, the system is inducible using

genetically modified trypanosomes that contain the T7 polymerase and tetracycline repressor (TetR). When tetracycline is added to the culture, the TetR is released from the tetracycline operator upstream of the integrated RNAi vector, which results in the synthesis of dsRNA by the T7 polymerase that is constitutively expressed (Wang *et al.*, 2000). In Trypanosomes two endonucleases of the RNA III family (dicers) have been identified. They cleave dsRNA's into duplex small interfering RNA's (siRNA's). Second endonuclease called argonaute (slicer) has been proven to be present in these parasites. It forms a complex with a single-stranded guide siRNA's and cleaves the mRNA transcript which in turn cannot be translated (Barnes *et al.*, 2012).

3.4.2 RNAi construct

A 485bp region of the *T. brucei* SDH1 gene was amplified by PCR from genomic DNA using primers showed in table 1. The resulting PCR product was then cloned into the p2T7-177 RNAi vector that contains head-to-head T7 promoters to synthesis dsRNA and the selectable antibiotic resistance marker phleomycin (Figure 9).

Table 1. List of used oligonucleotides.

Name	Sequence
Forward primer	**GATGGATCC**CTCTGGGCTTCGTGCCGCAA
Reverse primer	**GGAAAGCTT**TGCCACGACAACAGCCGTCC

3.4.3 Region of SDH1 (Tb927.8.6580) used for RNAi

ATGCTACGGCGTTCTTTTAACCGTCTCGCCTCACACCTCAGCAAGGCGTACCCCGTGATCGATC
ATACGTTTGACTGCGTGGTAGTCGGTGCAGGGGGCTCTGGGCTTCGTGCCGCAATGGGTGTTG
CCGCCTCGGGTTATAATGTGGCATGCGTCTCCAAGTTATATCCCTCCCGTTCCCACACAATTGC
GGCTCAGGGAGGTATCAACGCTGCTCTCGGAAATTGCGAGGAGGATGACTGGCGTTGGCATGT
GTATGATACAGTGAAGGGAAGTGATTGGTTAGGTGACCAGGATGCAATTCAGTACATGTGTCA
GGAAGCACCTTGCGTGGTGTCGGAATTGGAGAGCATGGGTCTTCCATTTCTCCGTACAAAGGA
TGGCTTCATCTACCAGCGAGCATTCGGTGGACAGTCTATTCACTATGGTGGGAAGCAGGCAAG
GCGGACATGTGCGGCATCCGATCGCACGGGGCATGCGATGTTGCACACACTGTATGGCCAGTC
CTTCCAGTACGGAGTGAATTTCTTTAACGAATATTATTGTCTGGACTTGATGGTGGAGGACGGC
TGTTGTCGTGGCATTGTTGCGATGAGCATAGACGATGGTACTATCCACCGTTTCCGCTCAAAGT
ATACCATCCTTGCAACGGGTGGGTATGGTCGGTGCTGGTTCACAACCACCAGTGCTAAGTCAT
GCACGGGTGATGGAACAGCGATGGTGGCTCGTGCCGGTTTGGCCGCAGAGGATATGGAGTTTG
TGCAGTTCCATCCGACGGGTATTTATGGACCAGGAGTTTTAATTACTGAGGGGTCACGAGGTG

AGGGAGGTTACCTTATTAACAGCGAGGGGGAGCGTTTCATGGAGCGGTATGCTCCGAAAGCG
AAGGATCTGGCATCTCGCGATGTGGTGTCGCGTGCCATCACTCTCGAACTGCTCGCCGGTCGT
GGTTGTGGGCCAAAGAAGGATCATGTTCTTCTTCAGTTACATCACCTCCCACCAGAGCAGCTTC
GCCAAAAGCTTCCGGGTATCTCTGAGAGCGCTCACATATTTGCTGGTGTGGATGTAACGAAAG
AATCCATTCCCATTGTGCCCACCGTTCACTACTCCATGGGTGGCGTCCCCACGCTTTGGACGGG
TGAGGTCGTAAACCCACGCAATGGTGATGACGATGCGATTGTACCGGGTCTCCTTGCGGCAGG
GGAGTGCGCTTGCGCGAGCGTTCATGGCGCTAATCGGCTGGGCGCCAACTCGCTGCTGGACAT
TGTGGTGTTTGGTAAGTCGTGCGCCAACACCGTCATTTTTAACCTAACGAAAGAGGGACGGGC
GCAACCCGAGTTGCGATCAGATGCAGGTGAGAGTTCCATTGCTGATCTTGACAAAATCCTTCA
TAATAAGGGTGATATCCCCGTTGCCCGCATTCGTGAGCGCATGAAGGAAACAATGGCTCTCTA
CGCTGCCGTGTTCCGGACGGAGGAGAGCATGCTTAAGGGCCAAGCAATCATCGAGGAATGCT
ACAGGGATTACTCACATGTTTTCGTCCACGACAAGTCTCCAGTATGGAACAGCAACCTCATTG
AGGCACTTGAGTTACGGAATTTACTTTACAACGCACTCATGACAATCGCTAGTGCGGCAGCGC
GGCGGGAGTCCCGTGGGGCCCATGCGCGTGACGACTACCCGGAGCGGGATGACCACAACTGG
ATGAAGCACACGCTTGCGTACATTAATGATAAGGAGGGTAAAGCGAAACTGGCTTACCGCCGT
GTGCACAGTGAGATGTTGACAAGTGAATTAGATAGCATTCCGCCAGCGAAGCGCGTCTACTAG

Figure 9. TbSDH1 p2T7-177 RNAi vector. Created in Geneious.

3.4.4 *E. Coli* transformations

Competent XL-1 blue cells were gently thawed on ice for 20 minutes. The construct containing the SDH1 gene was added and allowed to coat the cells while incubating on ice for another 10-20 minutes. The cell/DNA mixture was placed in a water bath (42°C) for 45 seconds to heat shock the cells, which induces them to take up the foreign DNA. The cells were then immediately put on ice for 2 minutes and allowed to recover. SOC (2 % tryptone, 0,5 % yeast extract, 10 mM NaCl, 2,5 mM KCl, 10 mM MgCl2, 10 mM

MgSO4, 20 mM glucose), a rich bacterial media, was added and the cells were placed in a shaking 37°C incubator for 1 hour. The transformed cells were then spread on an LB agar plate (1% NaCl, 1% peptone, 0.5% yeast extract, 1.5% agar) with ampicilin (100µg/ml) and left growing in an incubator overnight at 37°C. Plasmid DNA was isolated from 3-5 bacterial colonies using GenElute™ Plasmid Miniprep Kit (Sigma). The DNA was then digested with restriction enzymes and the resulting DNA fragments were analyzed on a 1% agarose gel. Positive clones were sequenced to confirm the correct insertion of the SDH1 RNAi fragment into the vector.

3.4.5 Transfection of *T. brucei* PF

The PF *T. brucei* strain 29-13, which are genetically engineered to constitutively expresses T7 RNA polymerase and tetracycline repressor were used for transfections (Motyka and Englund, 2004). These cells are grown in SDM-79 media containing the antibiotics neomycin (Neo) and hygromycin (Hyg) to selectively pressure the cells to retain the T7 polymerase and TetR, respectively. 10 ml of mid-log culture was harvested ($1x10^7$ cells per ml) by spinning them down at 1300g, 4°C, 10 minutes. The cell pellet was washed twice with 10 ml ice cold CytoMix buffer (25mM HEPES pH 7.6, 120 mM KCl, 0.15 mM CaCl2, 10 mM K_2HPO_4/KH_2PO_4 pH 7.6, 2 mM EDTA, 5 mM $MgCl_2$, 6 mM glucose) and then resuspended in 1ml of CytoMix. 10-20 µg of linearized, sterile DNA was loaded into a 0,2cm gap cuvette (Electroporation Cuvettes Plus Model no. 620, BTX) and 0,5 ml of the cell suspension was added. The mixture was electroporated with one pulse (1600V, 25Ω, 50µF) using the ECM630 PrecisionPulseTM, BTX-Genetronics, Inc. Electroporator. Cells were resuspended in 6ml SDM79 medium containing Neo and Hyg and incubated overnight. After 18 hours, the selectable antibiotic (phleomycin) was added at a concentration of 1 µg/ml and the cells were serially diluted into a 24-well plate to facilitate the cloning of transfectants with the integrated RNAi vector.

3.4.6 Transfection of *T. brucei* BF

BF single marker strain derived from *T. brucei* 427 (Wirtz *et al.*, 1999) cells were used for transfection. These cells have the T7 polymerase and TetR integrated into the genome with only the selectable antibiotic resistance marker Neo. $3x10^7$ cells was harvested at 1300xg for 10 minutes at 4°C and then washed with PBS-G and resuspended in human T-cell nucleofactor solution (Amaxa) with supplement.. 10-12µg of linearized DNA was

added into the cuvette. The mixture was electroporated by ECM650 aparatus using X-001 setting. Cells were resuspended in 30ml HMI-9 medium (G) and serially diluted into a 24-well plate and incubated overnight. After 18 hours, the selectable antibiotic (phleomycin) was added at a concentration of 2,5 μg/ml.

3.4.7 Growth curves and western verification of RNAi cell lines

T. brucei PF cells were cultivated in 10 ml of SDM-79 (neo/hyg/phleo) with 10% FBS in a 25ml cultivating flask. Each day the cells were counted on the Z2 Cell Counter (Beckman Coulter Inc.) and then split to $2x10^6$ cells/ml density. 1μg/ml tetracycline was added to the induced cultures daily. Growth curves of the cummulative cell density were calculated for the tetracycline induced and noninduced cultures. The degradation of the targeted SDH1 protein was verified by western blot as described previously. *T. brucei* BF cells were cultivated in 10 ml of HMI-9 (neo/phleo) with 10% FBS in 25ml cultivating flask. Every day the cultures were counted on the Z2 Cell Counter, split to $2x10^5$ cells/ml density and the induced cultures were given tetracycline. RNAi clonal cell lines were verified by western blot at various time points of the RNAi induction.

3.5 Mitochondrial membrane potential

Cells were grown to log phase and then stained for 30 minutes with 60nM tetramethylrhodamine ethyl ester (TMRE) for *T. brucei* PF, BF, DK cells and 100nM for *L. donovani*. Positive controls were performed by simultaneously incubating 20μM trifluorocarbonylcyanide phenylhydrazone (FCCP). After the incubation, cells were harvested by spinning down at 1300xg for 10 minutes at room temperature, resuspended in 1ml PBS pH 7,4 and transfered into fluorescence-activated cell sorting (FACS) tubes. The cells were subsequently analyzed by the Canto FACS machine counting 10000 events and measuring data in PE channel.

3.6 ATP production assay

We performed an *in vitro* ATP production assay with a crude organellar preparation enriched with intact and charged mitochondria. The assay requires a complete oxidative

phosphorylation (OXPHOS) pathway as it uses succinate as the electron donor into the pathway via succinate dehydrogenase. As the electrons flow through the OXPHOS complexes, protons are pumped into the intermembrane space to create a membrane potential, which is then used to power the F_oF_1-ATP synthase. The ATP produced was then measured in a luciferase assay. The principle is shown in the scheme (Figure 10).

$1x10^8$ PF *T. brucei* 427 wt cells were harvested by spinning for 10 minutes at 1300xg at 4°C. The cell pellet was washed once in PBS and then resuspended in 500µl So-TE (20mM Tris-HCl pH 7,75, 2mM EDTA, pH 8, 0,6M D-sorbitol). 500µl So-TE + 0,03% digitonin was added and the tube inverted once before being placed on ice for 5 minutes. The sample was spun for 3 minutes at 7000rpm at 4°C. The supernatant containing the soluble cytosolic fraction was discarded and the organellar pellet was resuspended in 800µl of an ATP production assay buffer (20mM Tris-HCl pH 7,4, 15mM KPi pH 7,4, 10mM $MgSO_4$, 0,6M D-sorbitol, 0,25% fatty acid free BSA). 75µl of the suspension was aliqouted into a 1,5 ml eppendorfs. 1µl of the appropriate inhibitor was added and allowed to incubate on ice for 10 minutes. Then sodium succinate 5mM and ADP 67µM were added into each well. The plate was incubated for 30 minutes at room temperature before the reaction was stopped by the addition of perchloric acid 116mM. Samples were spun down at 13200rpm for 5 minutes at 4°C to precipitate out all of the proteins in the solution. 60µl of the supernatant containing the synthesized ATP was transfered to a new 1,5ml eppendorf tube, neutralized with KOH 25mM and incubated for 10 minutes on ice. The sample was spun down at 13200rpm for 10 minutes at 4°C to remove any residual precipitates. Finally, 10µl of the soluble sample was added to 40µl of 0,5M Tris-Acetate ph 7,75 in a new plate. The amount of ATP present in each well was measured by the Orion II aparatus after adding 50µl of a luciferase solution (ATP bioluminiscence assay kit HSII, ROCHE).

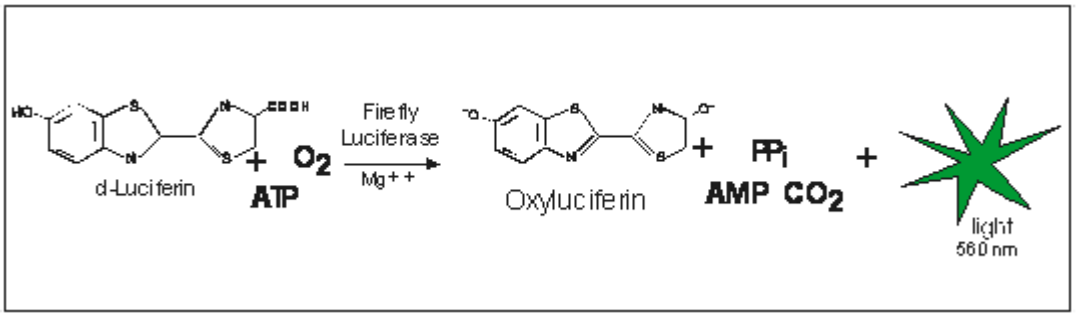

Figure 10. Bioluminescent Reactions Catalyzed by Firefly Luciferase. Firefly luciferase, using ATP, catalyses the two-step oxidation of luciferin to oxyluciferin, yielding light at 560 nm (http://www.biotek.com/resources/articles/dual-luciferase-assays.html).

3.7 ATPase assay with crude mitochondria

We utilized the Pullman assay to measure the amount of ATP hydrolysis in a crude mitochondrial preparation. This assay couples the hydrolysis of ATP with the oxidation of NADH, a reporter molecule that can be monitored spectrophotometrically at 340nm. Specific F_oF_1-ATPase inhibitors are used as controls to determine the percentage of ATP being hydrolyzed only by F_oF_1-ATPase in the crude fractionation. Mainly azide, an inhibitor of the F_1 ATP hydrolyzing moiety (Bowler *et al.*, 2006), and oligomycin, which binds the proton pore in the F_o moiety, were used. A scheme of the reaction is shown in figure 11.

Mitochondria were hypotonicaly isolated as described previously. The protein concentration was determined by a Bradford assay. Approximately 15µg of the crude mitochondria were incubated with bisphosphonium salts. To check if we measure the specific activity of F_oF_1-ATPase we used azide, which inhibits the ATP hydrolase activity of the mitochondrial F-ATPase by binding to the F_1 catalytic domain. The incubation lasted for 5 minutes and then the mix was transfered to 1ml UV cuvette containing an ATPase assay buffer (50mM Tris pH 8, 50mM KCl, 2mM $MgSO_4$), 200µM NADH (10mM Tris-Cl, pH 7,5, 50mM NADH), 1mM PEP, 5µl of lactate dehydrogeanse (Sigma) and 9µl of pyruvate kinase (Sigma). The reaction was then initiated by adding 2mM MgATP (400mM Tris-Cl, 200mM $MgSO_4$, 200mM ATP) to the UV cuvette already in the spectrophotometer, where the change of absorbance was measured at 340nm for 5 minutes. Specific ATPase activity of kinetoplastid lysate was calculated from the amount of NADH oxidized in 1 minute and related to the amount of the protein in the sample.

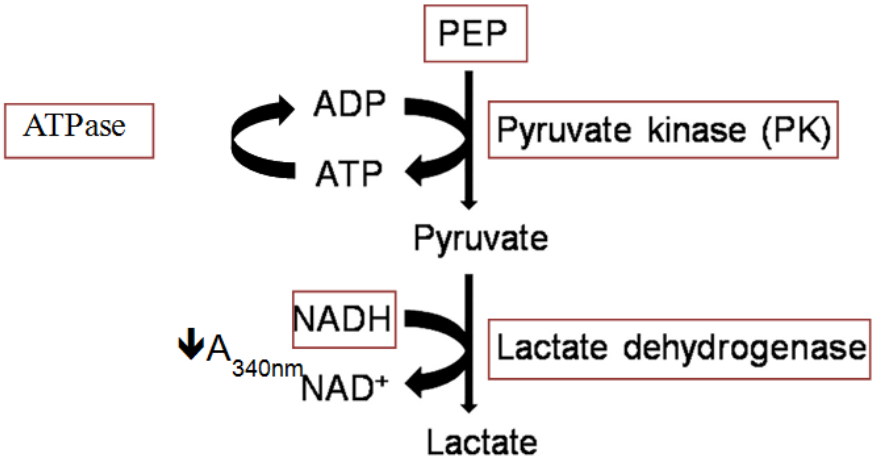

Figure 11. The two coupled reactions in a Pullman ATPase assay. The first reaction converts PEP into pyruvate by the pyruvate kinase. This produces ATP, which is then used as a substrate by the FoF1-ATPase, essentially coupling the two enzymes. The pyruvate is then futher reduced by NADH and lactate dehydrogenase to generate lactate. It is the oxidation of NADH that is measured spectrophotometerically. PEP-phosphoenolpyruvate, ATP-adenosine triphosphate, ADP- adenosine diphosphate, NAD+-nicotinamide adenine dinucleotide (NADH reduced form) (adapted from http://jb.asm.org/content/193/19/5386/F1.expansion.html).

3.8 ATPase assay with purified F1-ATPase

Cells were grown to 1-3x10^7 per 1ml, harvested by spinning down at 1300xg for 15 minutes at 4°C. The cell pellet was washed with SBG (150mM NaCl, 20mM glucose, 20mM NaH_2PO_4, 20mM Na_2HPO_4) and spun down at 1300xg for 10 minutes at 4°C. The pellet was resuspended in DTE and transfered to a dounce homogenizer. Cells were disrupted by 5-8 strokes. 60% sucrose was added immediately and mixed before the sample was spun down at 16000xg for 10 minutes at 4°C. The organellar pellet was resuspended in STM (250mM Sucrose, 20mM TRIS pH 8, 2mM $MgCl_2$). $MgCl_2$, $CaCl_2$ and DNase I were added, mixed and incubated on ice for 1 hour. An equal volume of STE was added and the samples were spun down for 10 minutes at 16000xg. The lysate pellet was resuspended in 70% Percoll and layered under the 20-35% Percoll gradient by a metal needle. Gradients were spun at 24000rpm for 1 hour at 4°C. Using 18 gauge needles and a 20cc syringe, the broad, opaque layer between the top (membrane fraction) and bottom (nuclear fraction) was collected and washed with STE 4 times (16000xg, 15 minutes).

Purified mitochondria were resuspended in buffer A (0,25M sucrose, 50mM Tris-HCl pH8, 1mM DTT). The suspension was sonicated on power 8.5 for 3x40 seconds, with an incubation on ice for 1 minute between sonications to prevent heating the sample.

Then the samples were further sonicated for 10x15 seconds bursts, again left on ice for 1 minute between the sonication (Sonicator 3000, Misonix, 19mm probe, 250watts). The submitochondrial particles were then pelleted overnight in an SW60Ti rotor at 23000rpm (52 000g) at 4°C.

The SMP pellet was resuspended in buffer B (0.25M sucrose, 50mM Tris HCl pH 8.0, 1mM DTT, 4mM EDTA, 2mM ADP). Chloroform, saturated with 2M Tris-HCl ph 8,5, was added to the pellet and then vigorously shook for 20 seconds. Immediately, the samples were centrifuged for 5 minutes at 8500rpm at room temperature. The top (light brown) layer was taken, leaving the middle (dark brown) and the bottom (chloroform containing) layers behind. The F_1 depleted SMPs and residual chloroform were removed by centrifugation in an SW28 rotor at 27 000 rpm for 30 minutes at RT, using chloroform resistant polyallomer tubes. The F_1 containing supernatant was carefully removed to avoid any chloroform contamination, blown with nitrogen for 15 minutes to remove all traces of chloroform. The F_1-ATPase was filtered, concentrated down to 750 µl and loaded on a Superdex 200 10/300 GL . The F_1 was purified on a FPLC using a specific F_1-column buffer (20mM Tris pH 8.5, 200mM NaCl, 1mM DTT, 4mM EDTA, 1mM ADP, 0.002% PMSF (optional)).

Activity was measured by the same procedure as described in section 3.7.

4 Results

4.1 Succinate dehydrogenase in trypanosomatids

4.1.1 SDH levels in trypanosomatids

Because the target of bisphosphonium salts in *Leishmania* was suggested to be succinate dehydrogenase (SDH), we explored the levels of this enzyme in *L. donovani*, *T. brucei* BF, PF and DK. First, we attempted to determine the steady state levels of a specific subunit of cII, SDH1, which contains the cofactor FAD that gets reduced by the electrons donated by succinate. Our original western blot analysis was performed with whole cell lysates, but there was no detection of SDH1 in BF. Therefore, we decided to run 50ug of protein from isolated mitochondria on SDS-PAGE (Figure 12).

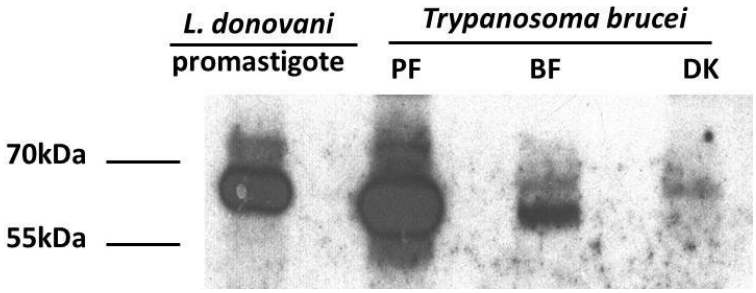

Figure 12. SDH levels in trypanosomatids. Mitochondria were isolated from equal numbers of cells from *L. donovani* (Ld) promastigotes and *T. brucei* (Tb) PF (PF) or BF (BF) or DK diskinetoplastic (DK). Same amount of proteins were loaded on a 12% SDS PAGE for each sample. After transfer to a PVDF membrane, the blot was probed with a rabbit antibody raised against a peptide of T. brucei SDH1.

Under these conditions, the correct size band (66 kDa) for the SDH1 protein was detected. The highest levels of expression are seen in PF *T. brucei* and to a lesser extent in the promastigote *L. donovani*., Much lower amounts of the cII subunit were detected in the BF *T. brucei* and almost nothing was detected in the DK cells. While equal amounts of total mitochondrial proteins were loaded for each sample, there is no reasonable loading control to include for the various life cycle stages of different trypanosomatid species. Therefore, these samples were run on BioRad's TGX stain-free precast gels that allow you to visualize all proteins with UV light from the Bio-Rad ChemiDoc instrument (Figure 13). These results consistently indicate similar levels of overall protein content for PF, BF and DK *T. brucei* mitochondrial samples. Furthermore, since these samples were analyzed repeatedly with similar results, the decreased SDH1 signal in BF and DK *T. brucei* is significant and not a result of uneven loading.

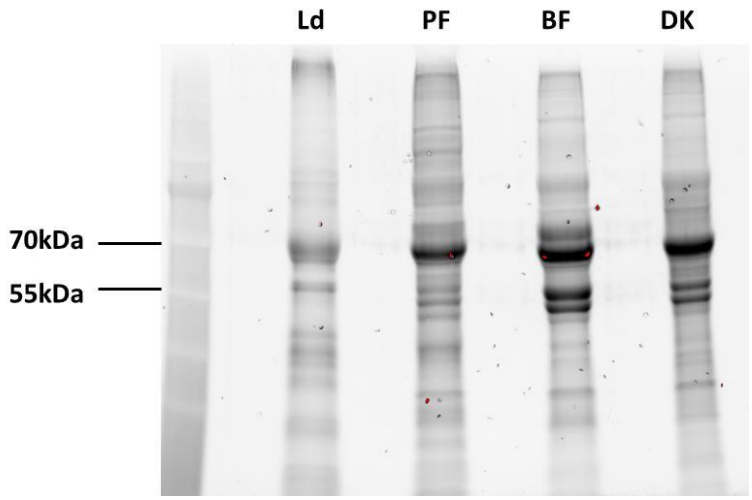

Figure 13. SDH levels in trypanosomatids - stain-free gel.

Interestingly, each stain-free gel containing the *L. donovani* mitochondrial sample appeared to have significantly less overall protein compared to the *T. brucei* samples, even though 50ug of protein were loaded for all. There are two possible reasons for this discrepancy, both center on the abundance of particular amino acids detected by either the Bradford assay or the stain-free technology. Since coomassie predominantly interacts with the amino acids arginine, lysine and histidine, it might be possible that these amino acids are overrepresented in *L. donovani* mitochondria and thus inflate the apparent abundance of all proteins as measured by a Bradford assay. On the other hand, the stain-free technology utilizes trihalo compounds that react with tryptophan, so if this residue is significantly underrepresented in *Leishmania* mitochondrial proteins it would seem as if less proteins were loaded. Either way, there is a strong signal for SDH1 that most likely is very comparable to the signal detected in PF *T. brucei* if equal loading were achieved.

Overall, these results are in agreement with the reduced mitochondrial function in both BF and DK *T. brucei*.

4.1.2 Assembly of succinate dehydrogenase and its enzymatic activity

To gain better insight about the significance of the function of cII on respiration, we analyzed the levels of assembled succinate dehydrogenase in trypanosomatids by performing high resolution clear native electrophoresis (Figure14).

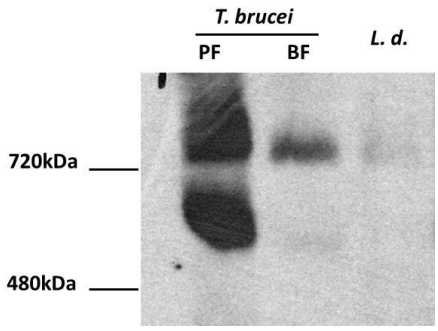

Figure 14. High resolution clear native electrophoresis demonstrates the levels of assembled respiratory complex II. Mitochondria were isolated from *T. brucei* PF & BF cells and *L. donovani* promastigotes. 50ug of mitochondrial protein were loaded for each sample onto a high resolution clear native (hrCN) PAGE, which was blotted and probed with the TbSDH1 peptide antibody. PF procylic form, BF bloodstream form, L.d. *Leishmania donovani* promastigotes.

The expected band of ~500kDa (Acestor *et al.*, 2011) is predominate in the PF *T. brucei* samples, but very faint in BF *T. brucei*. This correlates well with the steady state levels of SDH1 in these two life stages of *T. brucei*. However, the cII signal is undetectable in the *L. donovani* sample. One reason for this might be that the avidity of the *T. brucei* peptide antibody is weaker for this species of Trypanosomatid as the alignment of the peptide used to generate this antibody indicates in Figure 7, but this is not supported by the steady state SDH1 western analysis. More likely, as mentioned above, even though 50ug of total mitochondrial proteins were loaded for each sample, the *Leishmania* sample may be underrepresented. Furthermore, the SDH1 activity assays described below indicate that the antibody is not able to detect the native complex, possibly for steric reasons that don't apply to the *T. brucei* complex.

Interestingly, two bands were detected, suggesting that the complex may form a dimer or associate with another macromolecular complex like F_oF_1-ATP synthase (Kovářová *et al.*, 2013). However, since several other less prominent bands were detected on the mitochondrial lysates resolved by SDS-PAGE, most likely the higher band is the product of the antibody cross-reacting with another protein. This is further supported by the steady state levels of SDH1 and the activity measurements that follow.

Using a spectrophotometrical assay, we evaluated if the assembled complex is active (Table 2).

Table 2. SQR activity in trypanosomatids. Measured spectrophotometricaly as described in the methods section 3.3. Each measurement was performed in triplicates.

WT cells	SDH activity (%)
PF	100
Ld	60
BF	7
DK	2

Because the complex was most active in the PF of *T. brucei* it was set as 100% and the other samples were compared to this value. Each cell line was tested with the specific complex II inhibitor, malonate, to ensure that we measure the specific activity. P values were calculated using Student's t-test (<0,05 except DK value). These data closely correspond with the steady state levels of SDH1 in trypanosomatids, suggesting that respiratory complex II probably plays a much more important role in feeding electrons into the oxidative phosphorylation pathway in *L. donovani* promastigotes and PF *T. brucei* than in either the BF or DK *T. brucei* cells.

4.2 RNAi of *T. brucei* SDH1

To address if succinate dehydrogenase is essential for the viability of either life stage of *T. brucei*, we created two RNAi cell lines that knockdown the enzyme. We then measured the growth for 10 days of noninduced cells and RNAi induced cells.

4.2.1 *T. brucei* PF SDH1 RNAi

PF *T. brucei* are normally grown in a glucose rich (7.5mM) SDM-79 media. When PF SDH1 RNAi cells were grown in this media, we observed a very slight phenotype beginning around day 5 of tetracycline induced RNAi (Figure 15 left). PF cells can also be grown in SDM-79 with low glucose (3.5mM), which forces the cells to rely more on the oxidative phosphorylation chain for ATP production. Under these more physiologically relevant growth conditions, the same slight phenotype appears a little bit sooner – just after day 3 of RNAi induction (Figure 15 right). These data confirm that respiratory complex II is not essential for *T. brucei* PF.

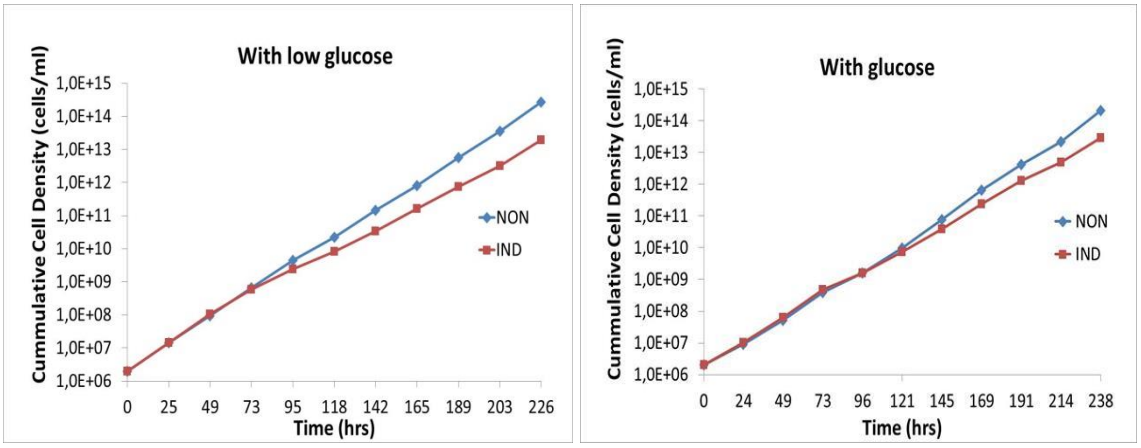

Figure 15. Growth curve of PF Tb SDH1 RNAi in media with glucose (left) and media with low glucose (right). PF *T. brucei* 29.13 cells were transfected with a linearized p2T7-177 vector containing a 485bp fragment of the TbSDH1 cds. The resulting clonal transfectants were then analyzed for a growth phenotype when RNAi was induced with 1ug/ml tetracycline. These growth curves are representative of several clones. NON noninduced cells, IND induced cells.

To verify the successful degradation of SDH1 in the RNAi cell line, we performed a western blot analysis with the Tb SDH1 peptide generated antibody (Figure 16). A size appropriate band disappears by day 1 (upper band). To confirm that the upper band is specific for SDH1, we washed the tetracycline out and observed the reappearance of the upper band within 48 hours.

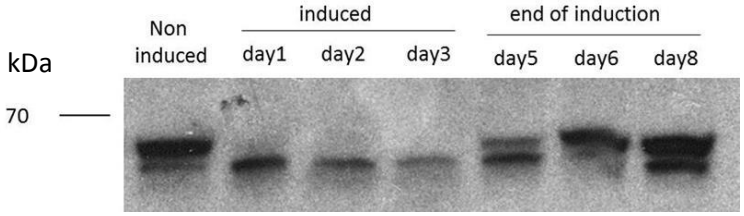

Figure 16. Western blot analysis of PF Tb SDH1 RNAi. Whole cell lysates made from equal amounts of cells were loaded on 12% SDS PAGE gel. After transfer, the PVDF membrane was probed with the SDH1 antibody.

SDH1 western blot analysis of a native gel was also performed (Figure 17). Interestingly, these set of native analyses in the PF SDH1 RNAi mitochondrial lysates only seem to detect a single band, which represents the lower expected band seen in previous native electrophoresis of mitochondria. This intensity of this band is dramatically decreased over time as the SDH1 RNAi is induced, indicating that the knockdown of a core succinate dehydrogenase subunit results in the disruption of the entire respiratory complex II. Therefore, this Tb SDH1 RNAi cell line could be used to evaluate if complex II activity is essential in PF cells. With reduced amounts of assembled succinate dehydrogenase, the activity of this enzyme was expected to decrease (Tab. 3). As a control, malonate was used as a specific inhibitor of complex II. The results correlate

nicely with the native electrophoresis analyses as the activity of the respiratory complex is diminished significantly as the amount of assembled complex is reduced (Figure 17).

Table 3. SQR activity in *T. brucei* PF SDH1 RNAi cell line. Assay was measured spectrophotometrically as described in method section 3.3. The activity of cells not treated with tetracycline was set as 100%. The assay was performed in triplicates. P values were calculated using Student's t-test (<0,05).

PF RNAi cl.1	% SDH activity
Non induced	100
Induced day 1	82
Induced day 3	35
Induced day 5	20
Non induced + malonate	17

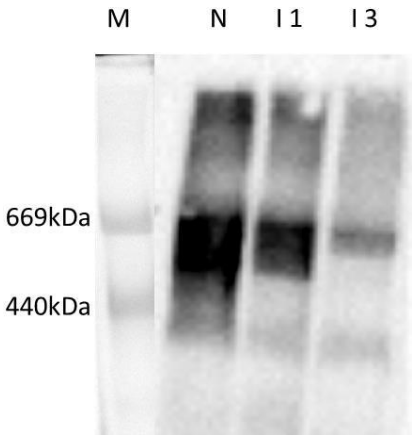

Figure 17. Native electrophoresis of the *T. brucei* PF SDH1 RNAi cell line. Cells were treated with tetracycline for 1 and 3 days. Equal amounts of protein from digitonin lysed mitochondria were run on a gradient polyacrylamide gel (3%-12%) and then transfered to a nitrocelulose membrane. The protein marker was separated and stained with Ponceau S. The membrane was probed with the primary SDH1 antibody. M marker, N noninduced, I1 induced day 1, I3 induced day 3.

To determine if the disabled function of complex II has any effect on the mmp, we measured this electrochemical gradient using a flow cytometry analysis with the dye TMRE that only stains charged mitochondria (Figure 18). As a control we used FCCP, a chemical uncoupler of respiration induced proton pumping and ATP synthesis. The resulting data conclusively indicate that the disruption of the complex doesn't change the membrane potential even after 5 days of induction, when the measured activity of the complex is similar to malonate inhibited samples. Taken all together, the data suggest that in PF *T. brucei* the flow of electrons through succinate dehydrogenase and into the oxidative phosphorylation pathway are minimal and not essential. Furthermore, this

indicates that respiratory complex II does not significantly contribute to the mmp in this life stage of *T. brucei*.

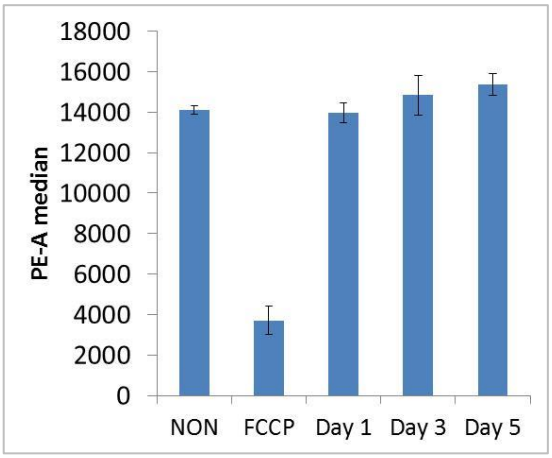

Figure 18. Tb PF SDH1 RNAi membrane potential. Assays were performed in triplicate. Error bars depict standard errors. P values were calculated using Student's t-test (<0,05).

4.2.2 *T. brucei* BF SDH1 RNAi

BF *T. brucei* lack a functional cytochrome mediated repiratory chain and a plant-like terminal alternative oxidase (TAO) acts as the final electron acceptor in order to maintain the mitochondrial redox balance (Chaudhuri *et al.*, 2002). Without several key components of the proton pumping respiratory chain, BF cells rely on F_oF_1-ATPase to hydrolyze ATP in order to maintain the mitochondrial potential (Brown *et al.*, 2006). To determine if the function of respiratory complex II is essential in BF *T. brucei*, we generated SDH1 knockdown in this life cycle of the parasite. When the SDH1 RNAi was induced with tetracycline, there was no growth phenotype (Figure 19 left). To verify that the SDH1 RNAi pathway was activated in these cells, western blot analysis of SDH1 steady state levels was performed (Figure 19 right). A prominent band of the expected size was observed in the noninduced cells, but this band was undetectable after just 24 hours of RNAi induction. Based on the previous RNAi results in PF *T. brucei*, we can assume that any assembled respiratory complex II has also been disrupted in these cells. Therefore, we conclude that succinate dehydrogenase is also not essential for the growth of BF *T. brucei*.

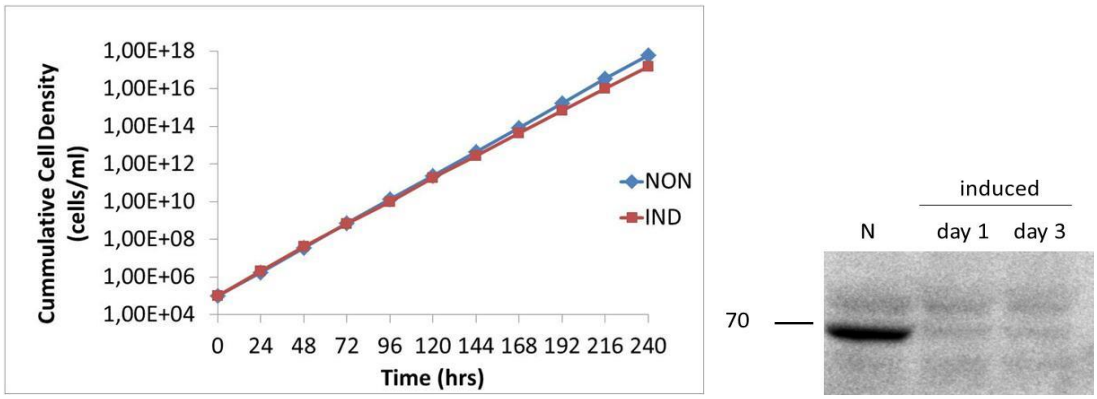

Figure 19. Growth curve of BF Tb SDH1 RNAi in media with glucose (left) and western blot analysis of this RNAi cell line (right). BF *T. brucei* SM cells were transfected with a linearized p2T7-177 vector containing a 485bp fragment of the TbSDH1 cds. The resulting clonal transfectants were then analyzed for a growth phenotype when the RNAi pathway was induced with 1ug/ml tetracycline. These growth curves are representative of several clones. NON noninduced cells, IND induced cells, N noninduced cells.

4.3 Verification of the effects of bisphosphonium salts on *L. donovani*

We tested two of the more potent bisphosphonium salts, AHI-9 and CD38, on *L. donovani* to see if we can get similar results as the Christopher Dardonville's lab. The previously calculated EC50 value for CD38 on *L. donovani* is 1,09±0,14µM. In our hands, the mmp was significantly decreased by both drugs at concentrations similar to the EC50 values (Figure 20). This suggests that the decreased membrane potential is an immediate effect of the compounds and likely the cause of death in the parasite as the membrane potential is essential for protein import (Geissler *et al.*, 2000) and thus mitochondrial activity. Interestingly, the mmp in *L. donovani* is slightly more sensitive to AHI-9.

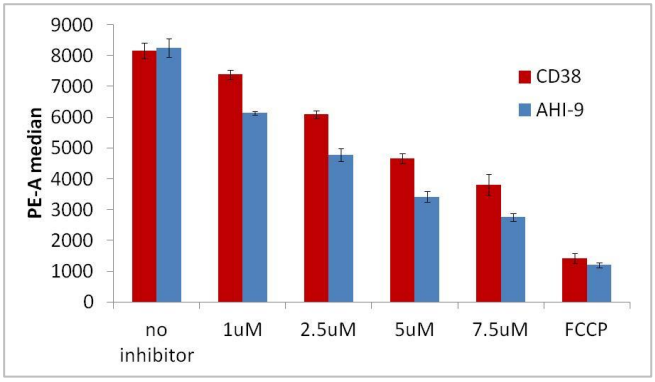

Figure 20. Effects of bisphosphonium salts on mmp in *L. donovani*. Cells were stained with 100nM tetramethylrhodamine ethyl ester (TMRE). As a positive control, cells were incubated with 20uM FCCP. Cells were harvested and analyzed by a Canto FACS machine counting 10 000 events and measuring data in PE channel. Assays were performed in triplicates. Error bars depict standard errors.

Next, we measured *L. donovani* SQR activity of succinate dehydrogenase from digitonin lysed mitochondria. Both CD38 (Figure 21 left) and AHI-9 (Figure 21 right) significantly inhibited the specific enzymatic activity, although at higher concentrations than the predicted EC50. Since it is known that these lipophilic cations likely concentrate in the mitochondria due to the membrane potential, it is possible that the higher concentrations needed to inhibit the activity in this assay is due to the fact that there are no intact and charged mitochondria to concentrate the drugs. Thus, the EC50 concentrations are slightly misleading for these *in vitro* activity assays without charged mitochondria and it would be very beneficial if we could measure the actual drug concentration in these charged mitochondria. However, because of this actual versus perceived drug concentration discrepancy, we can't rule out that the drugs targets multiple proteins, that in conjunction with the inhibition of succinate dehydrogenase, lead to cell death. Importantly, complex II was more sensitive to AHI-9.

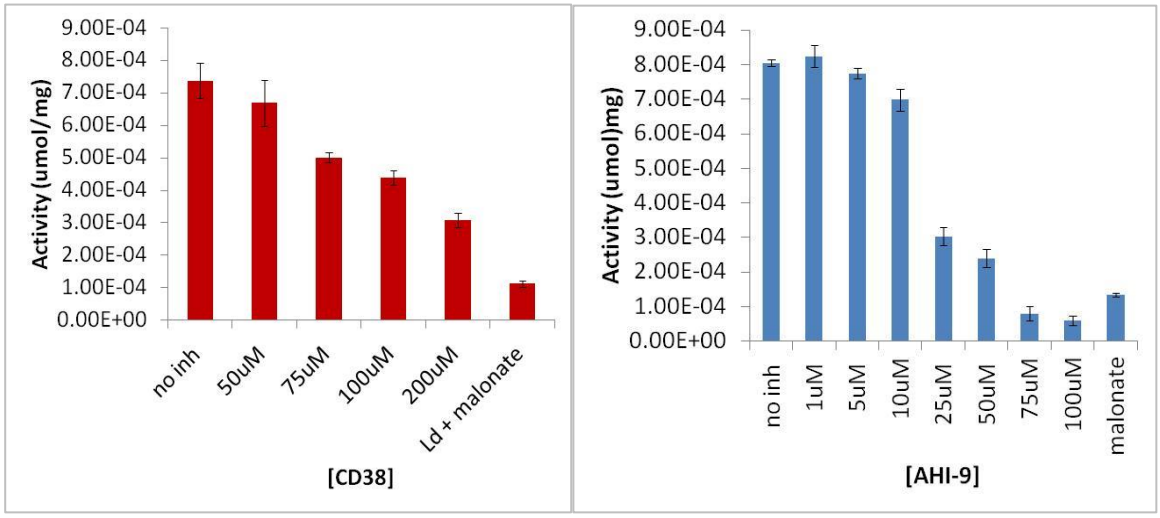

Figure 21. *L. donovani* SQR activity cells treated with CD38 (left) or AHI-9 (right). Assay were measured spectrophotometrically (see methods section 3.3). Experiments were performed in triplicates. Error bars depict standard errors.

4.4 Bisphosphonium salts mode of action in *T. brucei* PF

T. brucei is a closely related parasite to *L. donovani* and one would expect that the mechanism of action and the effects of bisphosphonium salts would be the same or similar, especially in PF *T. brucei* because it has similar mitochondrial activities. To answer that question, we measured the mmp and the activity of SDH after treating the parasites with either drug.

4.4.1 Effects of the drugs on mmp of *T. brucei* PF

Both CD38 and AHI-9 significantly decreased the mmp at concentrations similar to the EC50 (Figure 22). Again, since this assay is performed on live cells with charged mitochondria, these results suggest that the decreased membrane potential is an early effect of the drugs.

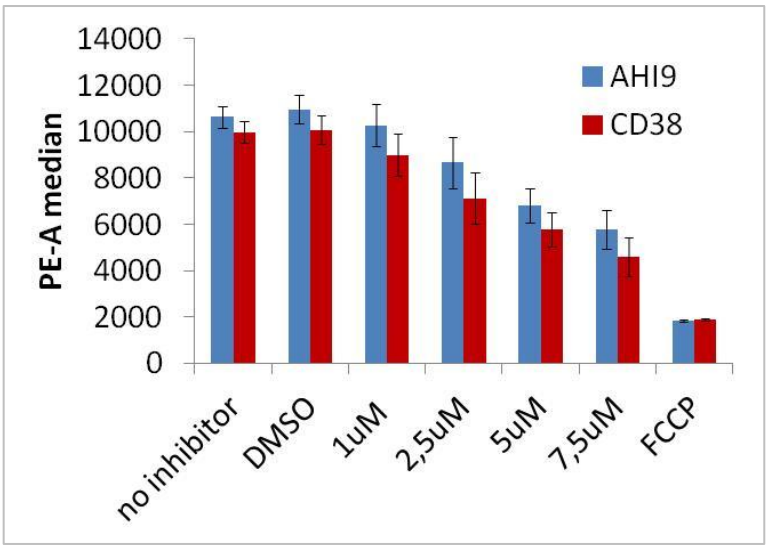

Figure 22. Mmp of *T. brucei* PF treated with CD38 and AHI-9. Cells were stained with 60nM tetramethylrhodamine ethyl ester (TMRE). Parasites incubated with 20uM FCCP served as positive control. Cells were harvested and analyzed by a Canto FACS machine counting 10 000 events and measuring data in the PE channel. Experiments were performed in triplicates. Error bars depict standard errors.

4.4.2 Effects of the drugs on succinate ubiquinone:oxidoreductase activity in *T. brucei* PF

The *in vitro* activity assay was again performed on lysed mitochondria from PF *T. brucei*. Interestingly, CD38 had almost no effect on SQR activity in the concentration range tested (Figure 23 left), while AHI-9 had an intermediate effect on inhibition at higher concentrations (Figure 23 right).

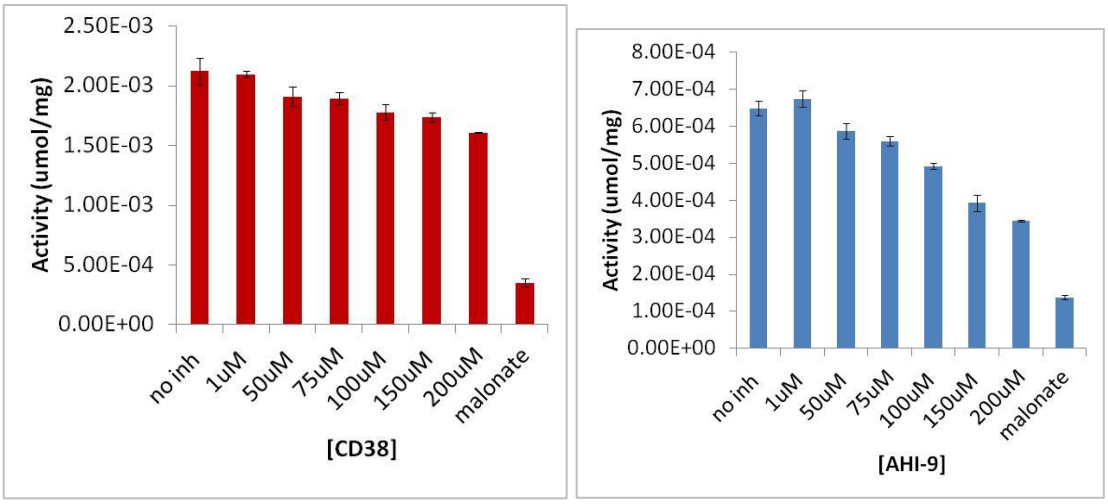

Figure 23. SQR activity of PF *T. brucei* treated with CD38 (left) or AHI-9 (right). Enzymatic activity was measured spectrophotometrically (described in the methods section 3.3). Assays were performed in triplicate. Error bars depict standard deviation errors.

4.4.3 Effects of the drugs on mmp of *T. brucei* BF and DK

Since the previous data suggest that the potent bisphosphonium salts may have other targets in addition to succinate dehydrogenase, we decided to measure the effects of the drugs on the mmp in BF and DK trypanosomatids. Because these cells lack functional cyctochrome containing respiratory complexes, the membrane potential is maintained in these cells by the hydrolysis of ATP by the F_oF_1-ATPase (Schnaufer *et al.*, 2006).

Our results indicate that both compounds severly effect the mmp in both BF (Figure 24 left) and DK (Figure 24 right) *T. brucei*. In fact, the active concentrations needed to produce a significant change were around 10 fold lower than those observed in PF *T. brucei*. EC_{50} values in BF for CD38 is 0,204±0,005µM and for AHI-9 0,082±0,01µM. This suggests that the F_oF_1-ATPase may be another target of bisphosphonium salts and quite possibly the actual mode of action in the infectious life stages of these parasites.

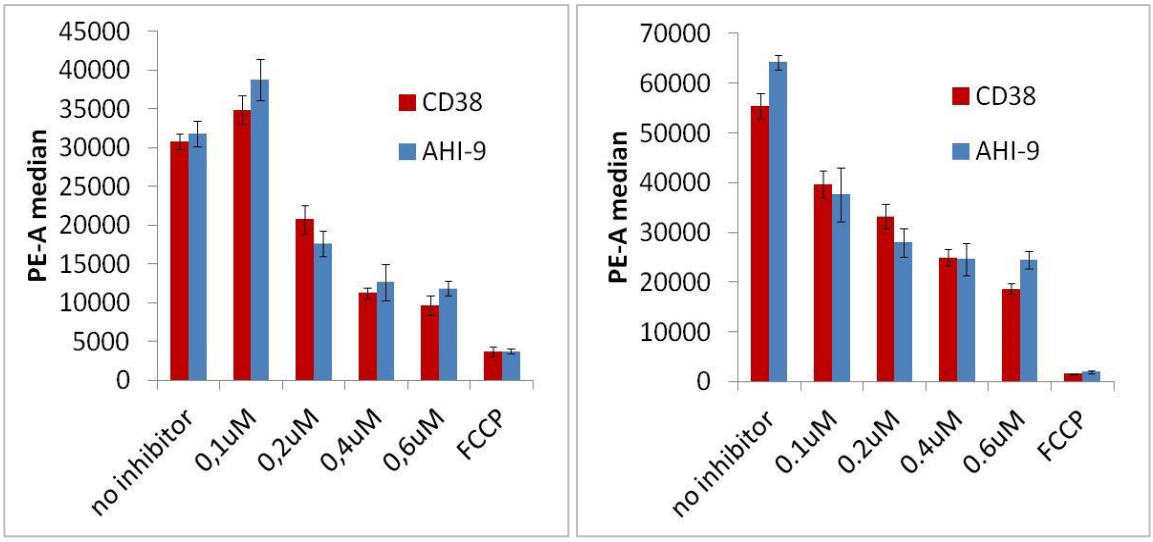

Figure 24. Mmp of *T. brucei* after using CD38 or AHI-9 in BF (left) and in DK (right). Cells were stained with tetramethylrhodamine ethyl ester (TMRE) at 60nM concentration. As positive control served cells incubated with FCCP (20uM [Final]). Cells were harvested and analyzed by Canto FACS machine counting 10 000 events measuring data in PE channel. Assays were performed in triplicates. Error bars depict standard errors.

4.4.4 Effects of the drugs on ATPase activity and purified F*1*-ATPase

To further explore if the bisphosphonium salts can indeed inhibit the activities of F_oF_1-ATPase/synthase, we first performed *in vitro* assays to measure ATP hydrolysis from either crude mitochondrial fractions or purified F_1-ATPase.

First we prepared crude mitochrial enriched fractions from PF *T. brucei* and measured the activity of respiratory complex V when treated with various concentrations of CD38 (Figure 25 upper) or AHI-9 (Figure 25 lower). Since there are many ATPases in these samples, they were treated with the specific F_1-ATPase inhibitor, azide. 1mM azide typically inhibits 30-40% of all the measured ATP hydrolysis activity in these samples. Increasing concentrations of both drugs approached the same inhibition as the azide control, albeit at much higher concentrations than their measured EC50. Again, these inflated values could be an artifact of another *in vitro* assay performed on lysed instead of intact and charged mitochondria that would be able to concentrate the drugs. Importantly, the same level of inhibition was detected when the crude mitochondria were treated with both azide and a bisphosphonium salt, indicating that both inhibitors are acting on the same target, F_oF_1-ATPase. Furthermore, the enzymatic activity was more drastically affected by AHI-9, which typically has a stronger killing effect on trypansomatids.

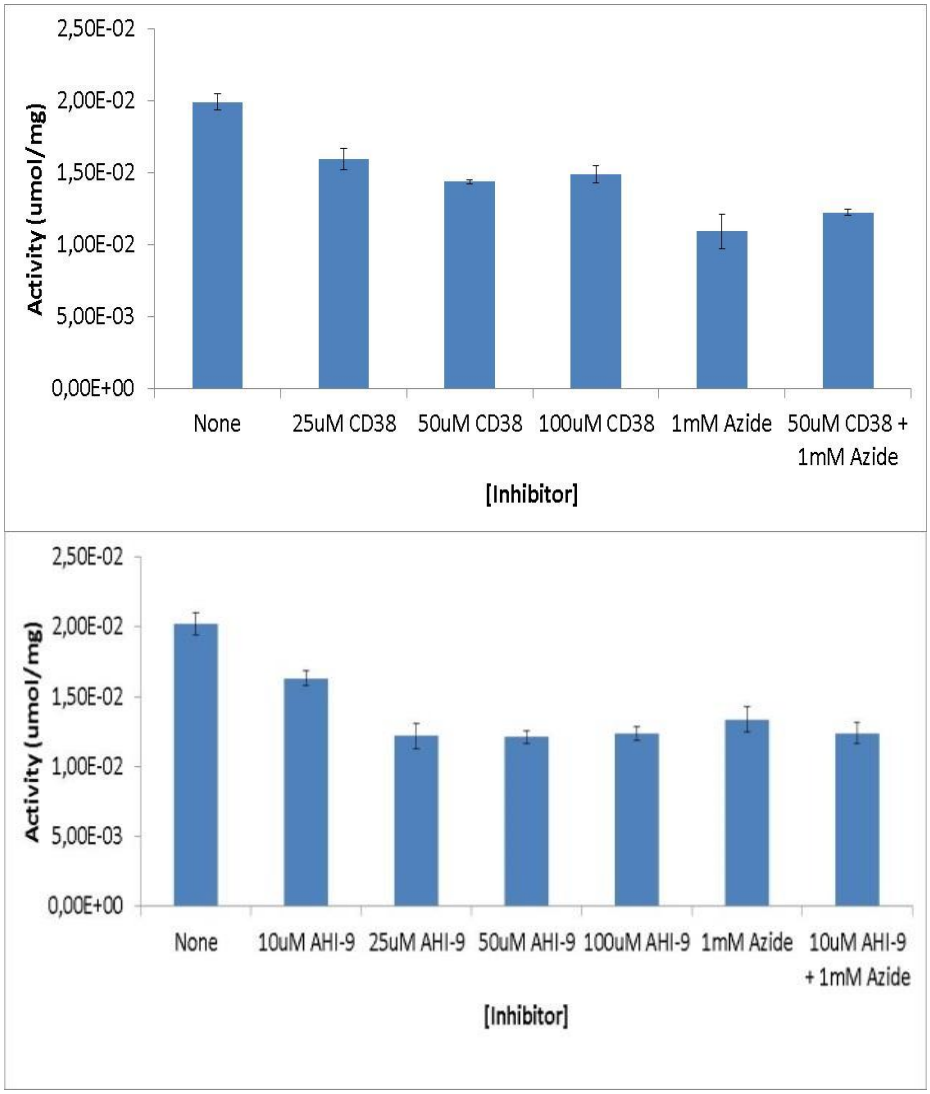

Figure 25. ATPase activity of mitochondrially enriched fractions of PF *T. brucei* 427 treated with CD38 (upper) and AHI-9 (lower). Approximately 15µg of hypotonically isolated mitochondria were incubated with their indicated inhibitors for 5 minutes and then transfered to an ATPase assay buffer. The change of absorbance was measured at 340nm for 5 minutes. Specific ATPase activity from mitochondrial lysates were calculated from the amount of oxidized NADH in 1 minute and related to the amount of total protein. Assays were performed in triplicate. Error bars depict standard deviation errors.

Since the preliminary data was promising, even if the crude mitochondrial samples contained many other ATPases, we repeated the assays on highly purified F_1-ATPase. Again, we obtain similar results to those obtained with the crude mitochondria (Figure 26). In this experiment, the azide inhibits almost 100% of the activity of the purified F_1-ATPase and increasing drug concentrations reduce the ATP hydrolysis activity in a linear range. Once again, AHI-9 appears to have significantly higher inhibition properties than

CD38. In fact, 20uM AHI-9 inactivates F_1-ATPase almost to the same extent as azide.

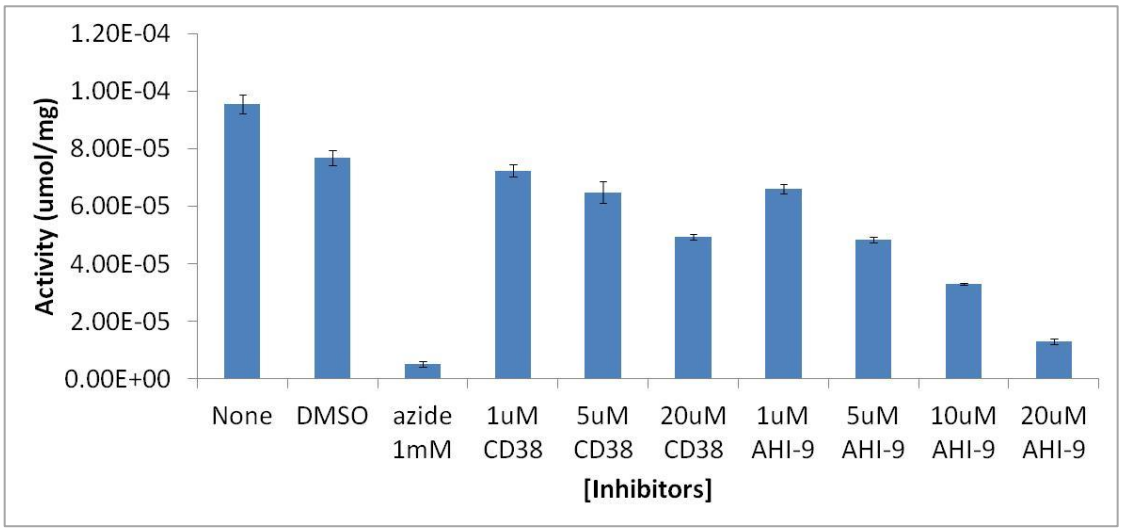

Figure 26. Activity of *T. brucei* purified F1-ATPase treated with both inhibitors. Performed as described above. Measured in triplicates. Error bars depict standard deviation errors.

4.4.5 Effects of the drugs on ATP production

To further evaluate the mechanism of action of bisphosphonium salts, we wanted to determine if they can effect the rate of ATP synthesis by F_oF_1-ATP synthase. This experimental set-up is not ideal to identify the exact biochemical target of the drugs because it relies on a complete and functional oxidative phopshorylation pathway, much like the original respiration assays performed in *L. donovani* by the Dardonville's lab. However, this assay is performed with intact, charged mitochondria and will give us some insight if both the ATP synthesis and hydrolysis activities of F_oF_1-ATPase can be affected by these compounds. Malonate, the specific inhibitor of succinate dehydrogenase, was used as a positive control as this complex receives the electrons from its substrate succinate and passes them along the oxidative phosphorylation pathway. Atractyloside is also added as a positive control as it is a specific inhibitor of the ADP/ATP carrier (AAC) (Kunji *et al.*, 2003), which is responsible for supplying the F_oF_1-ATP synthase with enough substrate. Not surprisingly, the results indicate that at concentrations similar to their measured EC50, CD38 inhibited ATP production at moderate levels, while AHI-9 almost completely inhibited ATP production (Figure 27). While this assay doesn't rule out respiratory complex II as a potential target, or even the AAC or the phosphate import carrier (PIC), it does suggest that an active mt membrane potential is important to these *in vitro* assays.

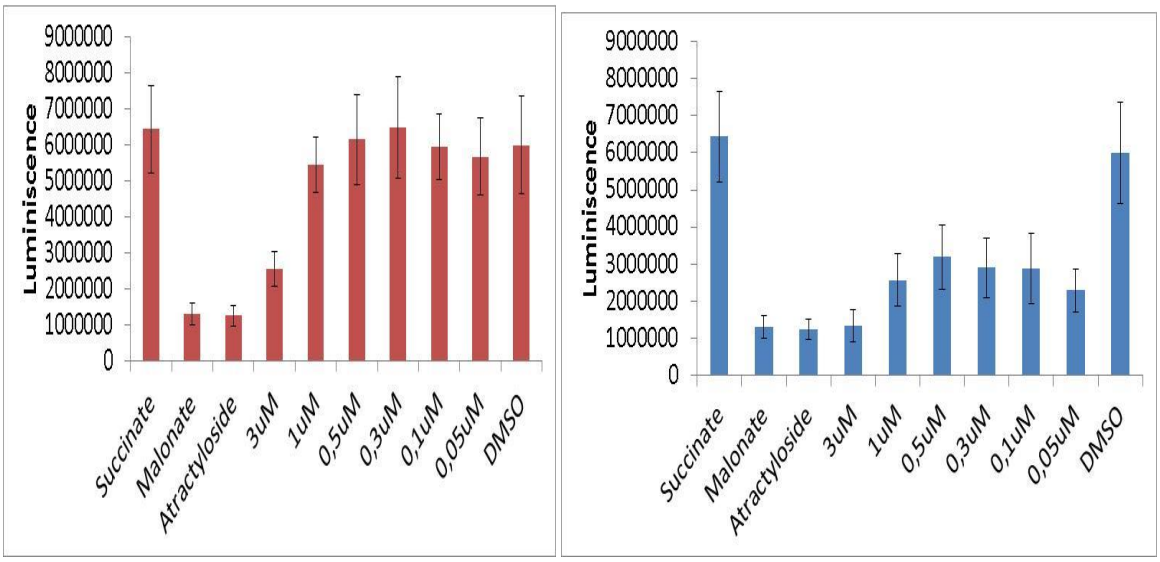

Figure 27. ATP production after using CD38 (left) or AHI-9 (right). We measured the bioluminescent reactions catalyzed by firefly luciferase. Firefly luciferase, using ATP, catalyses the two-step oxidation of luciferin to oxyluciferin, emitting light at 560 nm. A detailed describtion is in the methods section 3.6. Experiments were performed in triplicate. Error bars depict standard deviation errors.

5 Discussion

In 1977 it was first discovered that phosphonium salts are potent chemotherapeutics against *Trypanosoma cruzi* (Kinnamon and Steck, 1977). Two years later benzyltriphenylphosphonium salts were discovered to inhibit *Trypanosoma rhodesiense* (Kinnamon, 1979). However because of a lack of experience and information phosphonium salts got into attention after 30 years when new benzophenone-derived bisphosphonium salts were synthesized and tested against *Leishmania*. Higher killing activities were observed for the amastigote form of *Leishmania pifanoi* in comparison with promastigote form (Luque-Ortega, 2010). Moreover, there was a similar inhibitory potency of bisphosphonium salts (CD38, AHI-9) on the evolutionary close relatives, *T. brucei rhodesiense* trypomastigote (Taladriz *et al.*, 2012) and *T. brucei* 427 BF (Alkhaldi, 2012). The mode of action for these compounds has not been determined yet, but the compounds were revisited by the Dardonville lab in 2010 when they suggested that CD38 (compound 7) acts on succinate dehydrogenase. They drew upon the observations that there was some mitochondrial swelling and the membrane potential was significantly decreased at very low concentrations of the drugs. These results would suggest that the mode of action is either affecting a component of the oxidative phosphorylation pathway or the drug is acting as a kind of ionophore that depolarizes the membrane potential. The main experimental proof that identifies succinate dehydrogenase involves the measurement of the oxygen consumption rates. (Luque-Ortega, 2010). When they added CD38 to digitonized parasites it leads to a full inhibition of the oxygen consumption rate using succinate as substrate. They tried to add TMPD-ascorbate, an electron donor to cytochrome c and they observed restored oxygen consumption rate at 50% of the initial value that excludes cytochrome c oxidase (complex IV) as the site of inhibition and circumscribes the potential target upstream of cytochrome c. The oxygen consumption rate inhibited by CD38 was partially (33%) reinstated upon addition of R-glycerophosphate, a substrate of complex I. Consequently, this result ruled out complexes I and III as targets and supports complex II as the more likely target for this drug.

While the data certainly suggest that CD38 might be able to inhibit succinate dehydrogenase in *L. donovani*, it seems unlikely that this would be the mode of action for bisphosphonium salts in BF *T. brucei* because they lack cytochrome containing respiratory complexes and it is therefore assumed that complex II is largely inactive. Therefore, we decided to take advantage of the unique metobolic differences between PF

and BF *T. brucei* to provide greater insight into the mode of action for bisphosphonium salts in trypanosomatids. We decided to focus on the compounds CD38 and AHI-9, mainly because they have high trypanocidal activity and low toxicity on mammalian cells.

First, we were able to recapitulate the effects of the drugs on the membrane potential in promastigote *L. donovani*, so we decided to test if they could inhibit the specific activity of succinate dehydrogenase *in vitro*. While we are able to demonstrate a significant decrease in activity with the drugs, it was at concentrations 50x higher than the measured EC50. As mentioned in the results section, we propose that these lipophilic cations congregate in the mitochondria because the membrane potential creates a slightly negative charge in the matrix. This acts to effectively concentrate the compounds to levels that are higher than what is measured in the *in vitro* assays without charged mitochondria. If this premise is accepted, then the more interesting comparison lies between the *in vitro* inhibition assays of complex II in *L. donovani* versus *T. brucei*, where the inhibition is much less significant. It has been found that there are differences in the composition of this enzyme between the closely related trypanosomatids *T. brucei* and *T. cruzi* (Acestor *et al.*, 2011). Therefore, it is possible that there are some small structural variations between the *T. brucei* and *L. donovani* respiratory complex that would explain the decreased sensitivity in *T. brucei*. In fact, this is also supported by the fact that our peptide antibody to subunit SDH1 readily detects the subunit in SDS PAGE western blots of both *T. brucei* and *L. donovani* mitochondria, but not when used to probe native complexes. It would be interesting to further explore the structure of succinate dehydrogenase in these two closely related parasites and determine if the differences in the affinity of the bisphosphonium salts are the result of a steric hindrance either from compositional or structural changes.

With the methodology established, we next turned to *T. brucei* as a model to further explore the mode of action of these potent inhibitors. First, we verified that the bisphosphonium salts also cause a significant reduction in the mitochondrial membrane potential of PF, BF and DK *T. brucei* at concentrations similar to the calculated EC50 values. Therefore, it seems that this phenotype is an immediate downstream consequence of the inhibited target. Since respiratory complex II doesn't directly contribute to the membrane potential by pumping protons as it passes it's electrons to ubiquinone, we wanted to gain a better understanding of the role of this enzyme in supplying electrons to the oxidative phosphorylation pathway. As predicted, our native electrophoresis results

indicate that there is very little detectable succinate dehydrogenase in BF and DK *T. brucei* and that the measured *in vitro* activities of complex II are barely detectable compared to PF *T. brucei* and *L. donovani*. These results are in accordance with the significantly reduced mitochondrial activity in both BF and DK *T. brucei*, where the membrane potential is maintained by the hydrolysis of ATP by the F_oF_1-ATPase.

Our data strongly suggest that the ATP hydrolysis and synthesis activities of the F_oF_1-ATPase are inhibited by the the bisphosphonium salts CD38 and AHI-9. Interestingly, all of the biochemical analyses performed to date reveal a greater sensitivity to AHI-9, which correlates with the calculated EC50 values. It should be noted that the *in vitro* assays measuring ATP hydrolysis required concentrations of the compounds that are greater than the EC50, but the inhibition of the F_oF_1-ATPase is concentration dependent. Again, the mitochondrial membrane potential may lead to higher effective concentrations of the drugs than is added to the in vitro assay buffer. Unfortunately, we can't entirely rule out the possibility that the bisphosphonium salts also target either the AAC or PIC, which supply the required substrates for F_oF_1-ATPase, ATP and inorganic phosphate, respectively. However, the inhibition assays performed on just the highly purified F_1-ATPase, samples lacking the AAC or PIC, would indicate that any effects on these two carriers would be less significant since AHI-9 inhibited F_1-ATPase almost to the same levels as azide.

Therefore, it appears that the bisphosphonium salts can interact with both succinate dehydrogenase and F_oF_1-ATPase and the mode of action depends on the mitochondrial physiology of the parasite. Furthermore, the data would suggest that these compounds bind to the F_1-ATPase moiety because it inhibited the purified F_1-ATPase complex. For the fun of speculation, it would be interesting if these compounds bind to the catalytic ADP/ATP pockets between the alpha and beta subunits of F_1-ATPase and bind to a similar ADP/ATP binding pocket on succinate dehydrogenase. It has already been shown that the activity of cytochrome c oxidase can be regulated by the levels of adenylic nucleotides (Beauvoit *et al.*, 2001), so is it possible that the activity of succinate dehydrogenase is also regulated on this level? It would be plausible that when a cell needs to synthesize ATP, it upregulates the activity of complex II to start feeding more electrons into the oxidative phosphorylation pathway.

In summary, our data suggest that the potent bisphosphonium salt inhibitors most likely can interact with succinate dehydrogenase and F_oF_1-ATPase, but the mode of

action in BF *T. brucei* is most likely the inhibition of F_oF_1-ATPase to hydrolyze ATP and maintain the essential mitochondrial membrane potential.

6 Literature

ACESTOR, N., A. ZIKOVA, R. A. DALLEY, A. ANUPAMA, A. K. PANIGRAHI, K. D. HORVÁTH, Vladimir P. SKULACHEV, Henrik G. KJAERGAARD, Robin A. J. SMITH, Michael P. MURPHY a Christophe DARDONVILLE. *T. brucei* Mitochondrial Respiratome: Composition and Organization in PF. Molecular. 2011-09-08, vol. 10, issue 9, M110.006908-M110.006908. DOI: 10.1074/mcp.M110.006908.

ALKHALDI Abdulsalam Abdulhadi. (2012). Drug Development against Kinetoplastid Parasites. PhD thesis.

BARNES, Rebecca L., Huafang SHI, Nikolay G. KOLEV, Christian TSCHUDI, Elisabetta ULLU a John M. MANSFIELD. Comparative Genomics Reveals Two Novel RNAi Factors in *T. brucei* and Provides Insight into the Core Machinery. PLoS Pathogens. 2012-5-24, vol. 8, issue 5, e1002678-. DOI: 10.1371/journal.ppat.1002678.

BARRETT, M. P., & CROFT, S. L. (2012). Management of trypanosomiasis and Leishmaniasis. British medical bulletin, 104, p. 175–96. doi:10.1093/bmb/lds031

BARRETT, Michael P, Richard JS BURCHMORE, August STICH, Julio O LAZZARI, Alberto Carlos FRASCH, Juan José CAZZULO a Sanjeev KRISHNA. The trypanosomiases: a selfish altruism. The Lancet. 2003, vol. 362, issue 9394, p. 1469-1480. DOI: 10.1016/S0140-6736(03)14694-6.

BEAUVOIT, Bertrand, Michel RIGOULET, William L. HANSON a Willie L. CHAPMAN. Regulation of Cytochrome c Oxidase by Adenylic Nucleotides. Is Oxidative Phosphorylation Feedback Regulated by its End-Products?: new leads from a mouse model. IUBMB Life (International Union of Biochemistry and Molecular Biology: Life). 2001-9-1, vol. 52, 3-5, p. 143-152. DOI: 10.1080/152165401317316545.

BOWLER, M. W., M. G. MONTGOMERY, A. G. W. LESLIE a J. E. WALKER. How azide inhibits ATP hydrolysis by the F-ATPases: Technique, theory, and trouble shooting. Proceedings of the National Academy of Sciences. 2006-06-06, vol. 103, issue 23, p. 8646-8649. DOI: 10.1073/pnas.0602915103.

BRINGAUD, Frédéric, Loïc RIVIÈRE a Virginie COUSTOU. Adaptation to available carbon sources. Molecular and Biochemical Parasitology. 2006, vol. 149, issue 1, p. 1-9.

BROWN, S. V., P. HOSKING, J. LI a K WILLIAMS. ATP Synthase Is Responsible for Maintaining Mmp in BF *T. brucei*. Eukaryotic Cell. 2006-01-06, vol. 5, issue 1, p. 45-53. DOI: 10.1128/EC.5.1.45-53.2006.

BRUN, Reto, Johannes BLUM, Francois CHAPPUIS, Christian BURRI, Alberto Carlos FRASCH, Juan José CAZZULO a Sanjeev KRISHNA. Human African trypanosomiasis: a selfish altruism. The Lancet. 2010, vol. 375, issue 9709, p. 148-159. DOI: 10.1016/S0140-6736(09)60829-1.

CARABARIN-LIMA, Alejandro, María Cristina GONZÁLEZ-VÁZQUEZ, Olivia RODRÍGUEZ-MORALES, Lidia BAYLÓN-PACHECO, José Luis ROSALES-ENCINA, Pedro Antonio REYES-LÓPEZ a Minerva ARCE-FONSECA. Chagas disease (American trypanosomiasis) in Mexico: An update. Acta Tropica. 2013, vol. 127, issue 2, p. 126-135. DOI: 10.1016/j.actatropica.2013.04.007.

CHAPPUIS, François, Shyam SUNDAR, Asrat HAILU, Hashim GHALIB, Suman RIJAL, Rosanna W. PEELING, Jorge ALVAR a Marleen BOELAERT. Visceral Leishmaniasis: what are the needs for diagnosis, treatment and control?. Nature Reviews Microbiology. 2007, vol. 5, issue 11, p. 7-16.

CHAUDHURI, MINU, RITA SHARAN, GEORGE C. HILL, Eliška HOLZEROVÁ, Marek VRBACKÝ, Petr PECINA, Kateřina HEJZLAROVÁ, Katarína KĽUČKOVÁ, Jakub ROHLENA, Jiri NEUZIL, Josef HOUŠTĚK a Nagendra YADAVA. Trypanosome Alternative Oxidase is Regulated Post-transcriptionally at the Level of RNA Stability: Technique, theory, and trouble shooting. The Journal of Eukaryotic Microbiology. 2002, vol. 49, issue 4, p. 263-269. DOI: 10.1111/j.1550-7408.2002.tb00367.x.

DOSTÁLOVÁ, Anna and Petr VOLF. *Leishmania* development in sand flies: parasite-vector interactions overview.Parasites. 2012, vol. 5, issue 1

ESCH, K. J. a C. A. PETERSEN. Transmission and Epidemiology of Zoonotic Protozoal Diseases of Companion Animals. Clinical Microbiology Reviews. 2013-01-07, vol. 26, issue 1, p. 58-85. DOI: 10.1128/CMR.00067-12.

GEISSLER, A., T. KRIMMER, U. BOMER, B. GUIARD, J. RASSOW a N. PFANNER. Membrane Potential-Driven Protein Import into Mitochondria. The Sorting Sequence of Cytochrome b2 Modulates the Delta psi -Dependence of Translocation of the Matrix-targeting Sequence. Molecular Biology of the Cell. 2000-11-01, vol. 11, issue 11, p. 3977-3991. DOI: 10.1091/mbc.11.11.3977.

GUALDRÓN-LÓPEZ, Melisa, Ana BRENNAND, Véronique HANNAERT, Wilfredo QUIÑONES, Ana J. CÁCERES, Frédéric BRINGAUD, Juan Luis CONCEPCIÓN a Paul A.M. MICHELS. When, how and why glycolysis became compartmentalised in the Kinetoplastea. A new look at an ancient organelle: An update. International Journal for Parasitology. 2012, vol. 42, issue 1, p. 1-20. DOI: 10.1016/j.ijpara.2011.10.007.

HALL, James P. J., Huanhuan WANG, J. David BARRY a David HORN. Mosaic VSGs and the Scale of *Trypanosoma brucei* Antigenic Variation.PLoS Pathogens. 2013-7-11, vol. 9, issue 7, e1003502-. DOI: 10.1371/journal.ppat.1003502.

HANDMAN, E. Leishmaniasis: Current Status of Vaccine Development. Clinical Microbiology Reviews. 2001-04-01, vol. 14, issue 2, p. 229-243

HASKER, Epco, Pascal LUTUMBA, François CHAPPUIS, Victor KANDE, Julien POTET, Anja DE WEGGHELEIRE, Charles KAMBO, Evelyn DEPOORTERE, Bernard PÉCOUL, Marleen BOELAERT a Joseph Mathu NDUNG'U. Human African Trypanosomiasis in the Democratic Republic of the Congo: A Looming Emergency?. PLoS Neglected Tropical Diseases. 2012-12-13, vol. 6, issue 12, e1950-

KEDZIERSKI, Lukasz a C. A. PETERSEN. Leishmaniasis. Human Vaccines. 2011-11-01, vol. 7, issue 11, p. 1204-1214. DOI: 10.4161/hv.7.11.17752.

KENNEDY, Peter GE, Katherine FIGARELLA, Ewan T. MACLEOD a Susan C. WELBURN. Clinical features, diagnosis, and treatment of human African trypanosomiasis (sleeping sickness): a selfish altruism. The Lancet Neurology. 2013, vol. 12, issue 2, p. 186-194. DOI: 10.1016/S1474-4422(12)70296-X.

KINNAMON, KE, STECK, EA & RANE, DS. (1979). A new chemical series active against African trypanosomes: benzyltriphenylphosphonium salts. J Med Chem, 22, 452-455.

KINNAMON, Kenneth E., Edgar A. STECK, HANSON a Willie L. CHAPMAN. In search of anti-*Trypanosoma cruzi* drugs: new leads from a mouse model. Journal of Medicinal Chemistry. 1977, vol. 20, issue 6, p. 741-744. DOI: 10.1021/jm00216a001.

KOVÁŘOVÁ, Nikola, Tomáš MRÁČEK, Hana NŮSKOVÁ, Eliška HOLZEROVÁ, Marek VRBACKÝ, Petr PECINA, Kateřina HEJZLAROVÁ, Katarína KĽUČKOVÁ, Jakub ROHLENA, Jiri NEUZIL, Josef HOUŠTĚK a Nagendra YADAVA. High Molecular Weight Forms of Mammalian Respiratory Chain Complex II: Technique, theory, and trouble shooting. PLoS ONE. 2013-8-13, vol. 8, issue 8, e71869-. DOI: 10.1371/journal.pone.0071869.

KUNJI, E. R. S., Alisdair R. FERNIE, H. Ekkehard NEUHAUS, B. GUIARD, J. RASSOW a N. PFANNER. Projection Structure of the Atractyloside-inhibited Mitochondrial ADP/ATP Carrier of Saccharomyces cerevisiae: much more than a mitochondrial issue. Journal of Biological Chemistry. 2003-07-24, vol. 278, issue 39, p. 36985-36988. DOI: 10.1074/jbc.C300304200.

LAI, D.-H., H. HASHIMI, Z.-R. LUN, F. J. AYALA a J. LUKES. Adaptations of T. brucei to gradual loss of kinetoplast DNA: *Trypanosoma equiperdum* and *Trypanosoma evansi* are petite mutants of T. brucei. Proceedings of the National Academy of Sciences. 2008-02-12, vol. 105, issue 6, p. 1999-2004. DOI: 10.1073/pnas.0711799105.

LUN, Zhao-Rong, De-Hua LAI, Feng-Jun LI, Julius LUKEŠ a Francisco J. AYALA. *T. brucei*: two steps to spread out from Africa. Trends in Parasitology. 2010, vol. 26, issue 9, p. 424-427. DOI: 10.1016/j.pt.2010.05.007.

LUQUE-ORTEGA, J. Román, Peter REUTHER, Luis RIVAS a Christophe DARDONVILLE. New Benzophenone-Derived Bisphosphonium Salts as Leishmanicidal Leads Targeting Mitochondria through Inhibition of Respiratory Complex II. Journal of Medicinal Chemistry. 2010-02-25, vol. 53, issue 4, p. 1788-1798.

MORALES, J., T. MOGI, S. MINEKI, E. TAKASHIMA, R. MINEKI, H. HIRAWAKE, K. SAKAMOTO, S. OMURA, K. KITA, F. BRINGAUD a Christophe DARDONVILLE. Glucose-induced Remodeling of Intermediary and Energy Metabolism in Procyclic *T. brucei*: Composition and Organization in PF. Journal of Biological Chemistry. 2009-03-06, vol. 284, issue 11, p. 7255-7263. DOI: 10.1074/jbc.M806623200.

MOTYKA, Shawn A, Paul T ENGLUND, J. David BARRY a David HORN. RNA interference for analysis of gene function in trypanosomatids: Technique, theory, and trouble shooting. Current Opinion in Microbiology. 2004, vol. 7, issue 4, p. 362-368. DOI: 10.1016/j.mib.2004.06.004.

NOLAN, Derek P. a H. Paul VOORHEIS. Factors that determine the plasma-membrane potential in bloodstream forms of *T. brucei*.European Journal of Biochemistry. 2000, vol. 267, issue 15, p. 4615-4623. DOI: 10.1046/j.1432-1327.2000.01477.x.

NUNES, Maria Carmo Pereira, Wistremundo DONES, Carlos A. MORILLO, Juan Justiniano ENCINA, Antônio Luiz RIBEIRO, Pedro Antonio REYES-LÓPEZ a Minerva ARCE-FONSECA. Chagas Disease: An update. Journal of the American

College of Cardiology. 2013, vol. 62, issue 9, p. 767-776. DOI: 10.1016/j.jacc.2013.05.046.

ROBERTS, Larry S, Gerald D SCHMIDT and John JANOVY. Foundations of parasitology. 8th ed. Boston: McGraw-Hill Higher Education, c2009, p. 61-88. ISBN 0073028274.

ROSS, Michael P., Tatiana DA ROS, Frances H. BLAIKIE, Tracy A. PRIME, Carolyn M. PORTEOUS, Inna I. SEVERINA, Vladimir P. SKULACHEV, Henrik G. KJAERGAARD, Robin A. J. SMITH, Michael P. MURPHY a Christophe DARDONVILLE. Targeting lipophilic cations to mitochondria. Biochimica et Biophysica Acta (BBA) - Bioenergetics. 2008, vol. 1777, 7-8, p. 1028-1031. DOI: 10.1016/j.bbabio.2008.03.029.

SCHNAUFER, Achim, H. HASHIMI, Z.-R. LUN, F. J. AYALA a J. LUKES. Evolution of dyskinetoplastic trypanosomes: how, and how often?. Trends in Parasitology. 2010, vol. 26, issue 12, p. 557-558. DOI: 10.1016/j.pt.2010.08.001.

SCHNAUFER, G D CLARK-WALKER, A G STEINBERG a K STUART. The F1-ATP synthase complex in bloodstream stage trypanosomes has an unusual and essential function. The EMBO Journal. 2006-3-8, vol. 25, issue 5, p. 1175-1176. DOI: 10.1038/sj.emboj.7601013.

SIMARRO, Pere P., Jean JANNIN a Pierre CATTAND. Eliminating Human African Trypanosomiasis: Where Do We Stand and What Comes Next?. PLoS Medicine. 2008, vol. 5, issue 2, e55-.

TALADRIZ, Andrea, Alan HEALY, Eddysson J. FLORES PÉREZ, Vanessa HERRERO GARCÍA, Carlos RÍOS MARTÍNEZ, Abdulsalam A. M. ALKHALDI, Anthonius A. EZE, Marcel KAISER, Harry P. DE KONING, Antonio CHANA a Christophe DARDONVILLE. Synthesis and Structure–Activity Analysis of New Phosphonium Salts with Potent Activity against African Trypanosomes. Journal of Medicinal Chemistry. 2012-03-22, vol. 55, issue 6, p. 2606-2622. DOI: /10.1021/jm2014259.

TIELENS, A.G.M a J.J VAN HELLEMOND. Differences in Energy Metabolism Between Trypanosomatidae. Parasitology Today. 1998, vol. 14, issue 7, p. 265-272.

WANG, Z., Alisdair R. FERNIE, H. Ekkehard NEUHAUS, B. GUIARD, J. RASSOW a N. PFANNER. Inhibition of *Trypanosoma brucei* Gene Expression by RNA Interference Using an Integratable Vector with Opposing T7 Promoters: much more than

a mitochondrial issue. Journal of Biological Chemistry. 2003-07-24, vol. 275, issue 51, p. 40174-40179. DOI: 10.1074/jbc.M008405200.

WIRTZ, Elizabeth, Simone LEAL, Claudia OCHATT a GeorgeA.M. CROSS. A tightly regulated inducible expression system for conditional gene knock-outs and dominant-negative genetics in *Trypanosoma brucei*. Molecular and Biochemical Parasitology. 1999, vol. 99, issue 1, p. 89-101. DOI: 10.1016/S0166-6851(99)00002-X.

YANG, Ping-Chang, Tahrin MAHMOOD, J. David BARRY a David HORN. Western blot: Technique, theory, and trouble shooting. North American Journal of Medical Sciences. 2012, vol. 4, issue 9, p. 429-. DOI: 10.4103/1947-2714.100998.